Short title: CPuORF33 represses AtHB1 translation

[§]**Corresponding author**: Raquel Lía Chan. Instituto de Agrobiotecnología del Litoral CONICET-UNL, Centro Científico Tecnológico CONICET Santa Fe, Colectora Ruta Nac. Nº 168 km. 0, Paraje El Pozo. 3000 Santa Fe – Argentina

E-mail: rchan@fbcb.unl.edu.ar

Tel/Fax: 54-342-4511370 extension: 5018

Title: A uORF represses the transcription factor AtHB1 in aerial tissues to avoid a deleterious phenotype

Pamela A. Ribone[#], Matías Capella[#], Agustín L. Arce, Raquel L. Chan[§]

Instituto de Agrobiotecnología del Litoral, Universidad Nacional del Litoral, CONICET, Centro Científico Tecnológico CONICET Santa Fe, Colectora Ruta Nacional Nº 168 km. 0, Paraje El Pozo, (3000) Santa Fe, Argentina.

[#]These authors equally contributed to this work

One sentence summary: An upstream ORF encoded in an homeodomain-leucine zipper I gene and regulated by a chloroplast signal causes ribosome stalling in aerial tissues that had been exposed to light.

Responsible author for distribution of materials: Raquel Chan

Authors' contributions

Conceived and designed the experiments: PAR, MC, ALA and RLC. Performed the experiments: PAR and MC. Analyzed the data: PAR, MC, ALA and RLC. Performed the computational analysis: ALA. Conceived and wrote the paper: RLC

Funding information:

This work was supported by Agencia Nacional de Promoción Científica y Tecnológica (PICT 2012 0955 and PICT 2014 3300). PAR and ALA are postdoctoral CONICET Fellows, MC is a former CONICET Ph. D. Fellow and RLC is a career member of the same institution.

Abstract

AtHB1 is an Arabidopsis homeodomain-leucine zipper transcription factor that participates in hypocotyl elongation under short day conditions. Here we show that its expression is post-transcriptionally regulated by an upstream open reading frame (uORF) located in its 5' UTR. This uORF encodes a highly conserved peptide (CPuORF), present in varied monocot and dicot species. The Arabidopsis uORF and its maize homolog repressed the translation of the main ORF in *cis*, independent of the sequence of the latter. Published ribosome footprinting results and the analysis of a frame shifted uORF, in which the repression capability was lost, indicated that the uORF causes ribosome stalling. The regulation exerted by the CPuORF was tissue-specific and did not act in the absence of light. Moreover, a photosynthetic signal is needed for the CPuORF action since plants with uncoupled chloroplasts did not show uORF-dependent repression. Plants transformed with the native *AtHB1* promoter driving *AtHB1* expression did not show differential phenotypes, whereas those transformed with a construct in which the uORF was mutated exhibited serrated leaves, compact rosettes, and most significantly, short non-dehiscent anthers and siliques containing fewer or no seeds. We thus propose that the uncontrolled expression of *AtHB1* is deleterious for the plant and hence, finely repressed by a translational mechanism.

Introduction

Plants, as sessile organisms, have evolved complex traits to cope with the surrounding environment and show high resilience to external perturbations that are somehow buffered by the regulatory interaction of developmental networks. Transcription factors (TFs) play key roles in such networks by acting as mediators between the perception of environmental factors and the cellular responses.

Six percent of plant genes encode TFs, which are classified in different families and subfamilies (reviewed by Ribichich et al., 2014). This classification is mainly based on their DNA-binding domain structures. Among these families, the homeodomain-leucine zipper (HD-Zip) TF family has been assigned roles in the response to biotic and abiotic stresses, as well as in developmental processes (Capella et al., 2015a; Ribone et al., 2015a). The family has been divided into four subfamilies, denoted I to IV, based on structural and functional features. Members of subfamily I were identified in several plant species and related to different stress responses, but also with processes such as leaf senescence and morphology (Vlad et al., 2014), stem elongation, hypocotyl elongation, venation patterning and pollen hydration (Wang et al., 2003; Manavella et al., 2006; Ré et al., 2014; Capella et al., 2015b; Ribone et al., 2015b; Moreno Piovano et al., 2017). Besides the HD-Zip domain, HD-Zip I TFs contain conserved motifs in their carboxy- and amino-termini (Arce et al., 2011). *In vitro* and *in vivo* experiments in different plant species showed that the HD-Zip I carboxy termini have key functional roles (Hofer et al., 2009; Arce et al., 2011; Sakuma et al., 2013). A motif similar to the AHA (Aromatic and large Hydrophobic residues in an Acidic context) transactivation motif was identified at the end of the carboxy-termini and was functionally characterized for Arabidopsis AtHB1, AtHB7, AtHB12 and AtHB13 members (Capella et al., 2014).

Most Arabidopsis HD-Zip I proteins were resolved as pairs in phylogenetic trees. Some of these pairs exhibited cross regulation and overlapping functions in certain conditions (Ré et al., 2014; Ribone et al., 2015b). This was not the case for AtHB1 which belongs to clade III and does not have a paralog (Arce et al., 2011). This HD-Zip I TF was shown to interact with AtTBP2 both in yeast two-hybrid and *in vitro* pull-down assays (Capella et al., 2014). The expression of this gene was repressed in NaCl-treated plants and in plants subjected to low temperatures, but was induced by darkness (Henriksson et al., 2005). In tobacco plants grown in absolute darkness, *AtHB1* overexpression caused constitutive photomorphogenesis (Aoyama et al., 1995). More recently, it was demonstrated that *AtHB1* expression is significant in hypocotyls and roots and this expression is regulated by PIF1 (*Phytochrome-Interacting Factor* 1) to promote hypocotyl elongation under a short day regime (Capella et al., 2015b). The analysis of *athb1* and *pif1* mutants, as well as their double mutants, indicated that PIF1 and AtHB1 regulate genes involved in cell wall synthesis.

Notably, *AtHB1* overexpressor lines never exhibited expression levels higher than x5 the endogenous levels, suggesting a post-transcriptional regulatory mechanism. Such a mechanism was evidenced when *rdr6-12* mutant plants, which have non-functional small RNA silencing machinery, were transformed with the same constructs as wild type Col-0 plants. Those *rdr6-12*/*AtHB1* plants exhibited high transcript levels and differential phenotypes (Romani et al., 2016), indicating that a silencing mechanism is taking place when *AtHB1* is an overexpressed transgene.

It is well known that the 5'UTR of mRNAs can contain different regulatory elements such as loops, protein binding sites, intern segments for ribosome entry and uORFs (upstream Open Reading Frames; Somers et al., 2013). These uORFs are located upstream from the main ORF (mORF) and, following Kozak's model for translation initiation, their first AUG codon starting from the CAP, is recognized by the ribosome to commence translation. Hence, when a uORF exists, its AUG is the initiation codon triggering a less efficient mORF translation in most cases (Kozak, 1987; Kozak, 2002).

In eukaryotic organisms, about 20-50 % of the transcripts have uORFs. However, those that encode conserved peptides occur in less than 1 % of transcripts. In these cases, the uORF is called CPuORF (Conserved Peptide uORF; Jorgensen and Dorantes-Acosta, 2012). The analysis of Arabidopsis and rice transcriptomes allowed the identification of 26 different CPuORFs (Hayden and Jorgensen, 2007), most of which are present in regulatory genes. Though the function of the CPuORFs is not yet well studied, a few reports have indicated that these sequences modulate the translational efficiency of the downstream main ORF in combination with small signal molecules (Rahmani et al., 2009; Ivanov et al., 2010; Alatorre-Cobos et al., 2012; Guerrero-Gonzalez et al., 2014; Laing et al., 2015). For example, the translation of the bHLH transcription factor SUPPRESSOR OF ACAULIS5 LIKE3 (SACL3) is blocked by a uORF in the absence of thermospermine (Katayama et al., 2015). Genes that do not encode TFs, like the Arabidopsis polyamine oxidase-2, were also shown to be regulated by a uORF and, in this case, the amino acid sequence was crucial for this regulation (Guerrero-González et al., 2016). Similarly, a noncanonical uORF represses GDP-L-galactose phosphorylase (GGP), the major control enzyme of ascorbate biosynthesis when ascorbate concentration is high (Laing et al., 2015).

A uORF encoding a conserved peptide was previously identified in the 5'UTR of *AtHB1* and called CPuORF33 (At3G01472.1) (Hayden and Jorgensen, 2007). Thus, it is conceivable that *AtHB1* expression is regulated through mRNA translation. Indeed, by using *in vitro* translation approaches, it has recently been shown that many CPuORFs, including CPuORF33, have the ability to cause ribosomal arrest (Hayashi et al., 2017). However, the physiological role of CPuORF33 and whether its mechanism of action is also functional *in vivo* remain unresolved.

Here we show that *AtHB1* translation is repressed *in vivo* by a mechanism involving CPuORF33. Our results indicate that this element acts via a ribosome stalling mechanism, independently of the sequence of the mORF downstream of the uORF. The CPuORF33 exerts its repressive effect only in aerial tissues except in darkness. Moreover, the maize CPuORF33 homolog showed a conserved function. Finally, we show that such a fine and sophisticated regulation is essential for the plant in order to avoid aberrant and lethal phenotypes caused by the uncontrolled expression of *AtHB1*.

134

Results

AtHB1 has a conserved open reading frame in its 5' untranslated region

In 2007, Hayden and Jorgensen revealed the presence of a conserved encoded peptide upstream from the main coding sequence of *AtHB1*, located in its 5'UTR. To investigate if such a sequence/peptide has a biological function, we carried out an *in silico* analysis of AtHB1 homologs from other plant species. Using the AtHB1 protein sequence as a query against the NCBI non-redundant protein sequences database, a search with BLASTP allowed the retrieval of 45 different nucleotide sequences encoding AtHB1 homologs belonging to 43 plant species, including mono- and dicots (Supplemental Table 1). These homologous sequences were assessed for the presence of ORFs upstream of the mORF; only ORFs starting with ATG and containing at least 24 bp were considered. This analysis led to the identification of 44 different uORFs, all of them belonging to the previously identified group 14 (Hayden and Jorgensen, 2007). An alignment of these sequences indicated a high degree of conservation and a difference in peptide length between mono- and dicots (Figure 1). In monocot AtHB1 homologs, the peptide had 38 amino acids whereas in dicots the length varied between 29 and 30. Accordingly, a phylogenetic tree resolved two clades (Figure 1B). Nucleotide sequences were also conserved but to a lesser extent than the amino acid sequences (Supplemental Figure 1). A BLAST analysis performed using either the monocot or the dicot consensus peptide did not find any other plant peptide or protein with sufficiently high similarity.

The Kozak rule describes the optimal sequence around the initiator AUG for an efficient translation (Kozak, 1986) and has been verified by different studies (Zur et al., 2013). Important positions include position -3 with an A or G, and position +4 with a G, which can be summarized as (A/G)XXATGG. This rule is generally fit by the sequence context of AUGs from uORFs having a single initial AUG; as well as those AUGs aligned to them but belonging to uORFs having two initial AUGs (Supplemental Figure 2).

A further analysis of *AtHB1* (and its homologs) uORF sequences indicated that the length is another conserved trait, though other characteristics of these sequences were also interesting. For example, no overlap between the uORF and the mORF was observed in any case. Additionally, other properties of the sequence traits were assessed but no remarkable features were found. Among the tested properties were: the distances between the CAP and the uORF starting site and between the uORF stop codon and the mORF AUG, as well as the phase of the uORF and the mORF (Supplemental Figure 3). The high sequence similarity between species strongly suggested a regulatory role for the CPuORF33. However, no motifs or a strong indication of secondary structure were found for the encoded peptide (data not shown).

Figure 1

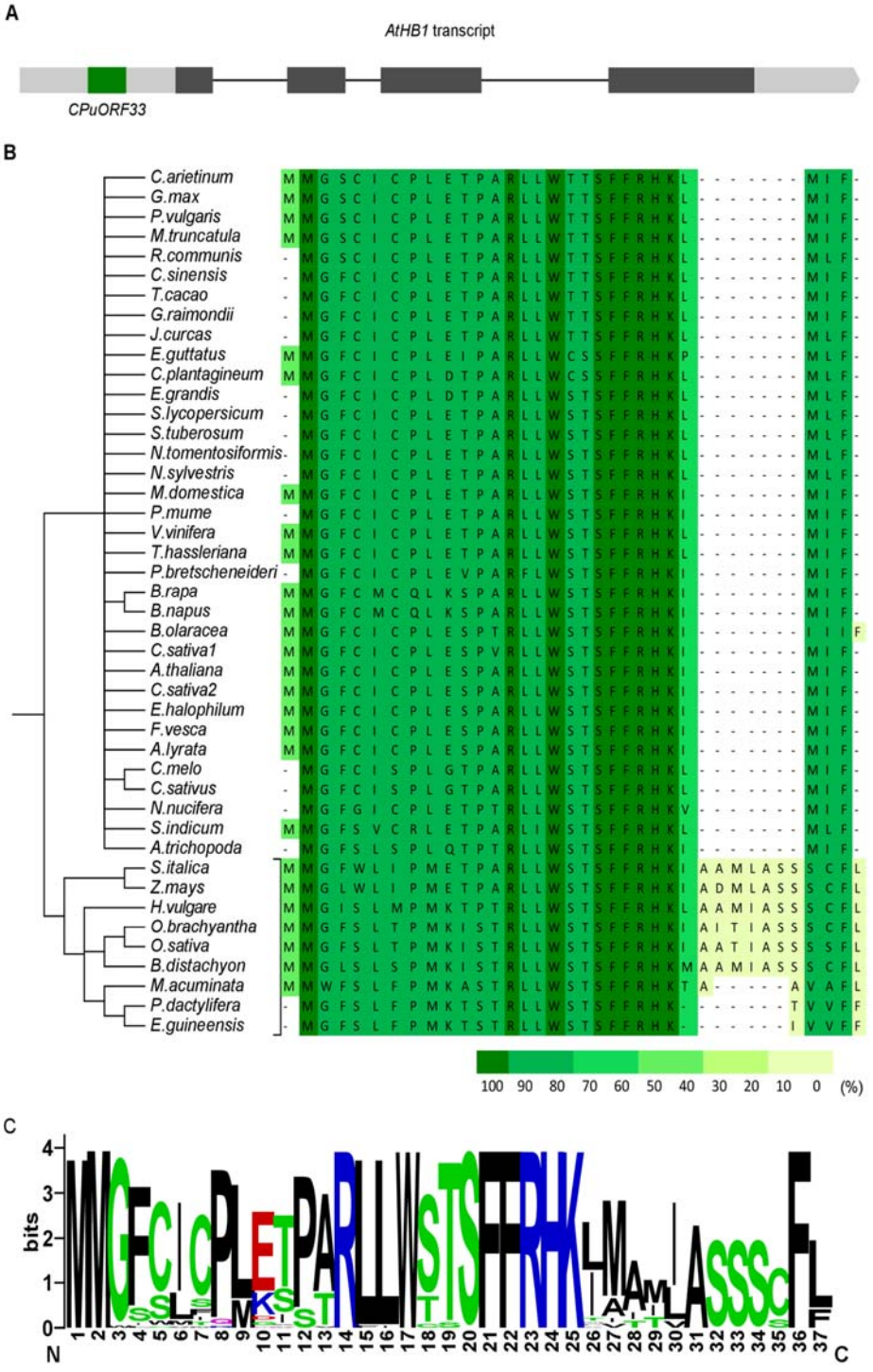

Figure 1. The predicted amino acid sequence of the CPuORF33 is highly conserved between species

A. Schematic representation of *AtHB1* gene. In grey, exons; in light grey, the 5' and 3'UTR; in red, the CPuORF33; and the introns in simple lines.

B. Left panel: Phylogenetic tree constructed using the predicted uORF amino acid sequences of 44 AtHB1 homologs from different species, available in public databases. Two main clades can be distinguished: dicotyledonous and monocotyledonous plants. Right panel: amino acid sequence alignment.

C. Amino acid sequence logo of CPuORF33. Sequence logo resulted from the alignment of the uORF amino acid sequences of 44 AtHB1 homologs from different species. Letters height corresponds to the frequency in the alignment.

CPuORF33 represses the expression of *AtHB1*

In light of the observations described above, we presumed that the CPuORF33 could play a regulatory role in the expression of *AtHB1* and its homologs. To address this hypothesis, two genetic constructs were generated (Figure 2A); in the first, the expression of the mORF of *AtHB1* was controlled by the 1415 bp upstream region from its ATG (*PromAtHB1:AtHB1*) and in the second, two point mutations (T→C) deleting both ATGs at the beginning of *CPuORF33* were introduced (*PromAtHB1mut:AtHB1*). These constructs were used to transform Col-0 *Arabidopsis thaliana* plants. T1 plants transformed with *PromAtHB1:AtHB1* did not exhibit phenotypic differences with respect to the WT control. In contrast, those transformed with *PromAtHB1mut:AtHB1* presented serrated leaves, short siliques with fewer or no seeds and a notable delay in bolting and entry to the senescent stage. A similar phenotype was observed in plants expressing *AtHB1* at high levels (Romani et al., 2016). Notably, the T2 generation of *PromAtHB1mut:AtHB1* plants recovered the WT phenotype (Figure 2B). To understand this observation, *AtHB1* transcript levels were quantified in both generations (T1 and T2) resulting high in T1 and clearly low in T2, even lower than in the WT, indicating that a silencing mechanism was in action (Supplemental Figure 4). For this analysis 15 single-copy lines were used; these lines were selected on the basis of herbicide resistance segregation in the T1 generation. Notably, this silencing observed in T2 plants was independent of CPuORF33, since both genotypes transformed with either *PromAtHB1:AtHB1* or *PromAtHB1mut:AtHB1,* exhibited lower transcript levels in T2 compared to T1.

Silencing mediated by small RNAs, and triggered by the overexpression of the transgene, has been already described for the HD-Zip I encoding genes *AtHB1* and *AtHB12* when driven by the constitutive 35S CaMV promoter (Romani et al., 2016), but this is the first time this silencing has been observed using the endogenous promoter.

To gain further insights into the molecular mechanism explaining the phenotypes regarding the CPuORF33, *rdr6-12* mutant plants were transformed with the same constructs. These plants have a mutation in the gene encoding the RNA-dependent RNA polymerase 6 (RDR6), which is absolutely necessary to display the small RNA mediated silencing cascade. As shown in Figure 2, the phenotype of the *rdr6-12* plants transformed with *PromAtHB1:AtHB1* was indistinguishable from that of plants transformed with the empty vector, whereas those transformed with *PromAtHB1mut:AtHB1* exhibited serrated leaves both in T1 and T2. Quantification of transcript levels in these new transgenic plants indicated high overexpression of the transgene in T1 and T2 (Supplemental Figure 4). These results strongly indicated that the small RNA silencing mechanism is independent of the uORF. In addition, *AtHB1* expression levels were similar comparing Col-0 and *rdr6-12* plants without further transformation (Supplemental Figure 5), indicating that the silencing

Figure 2

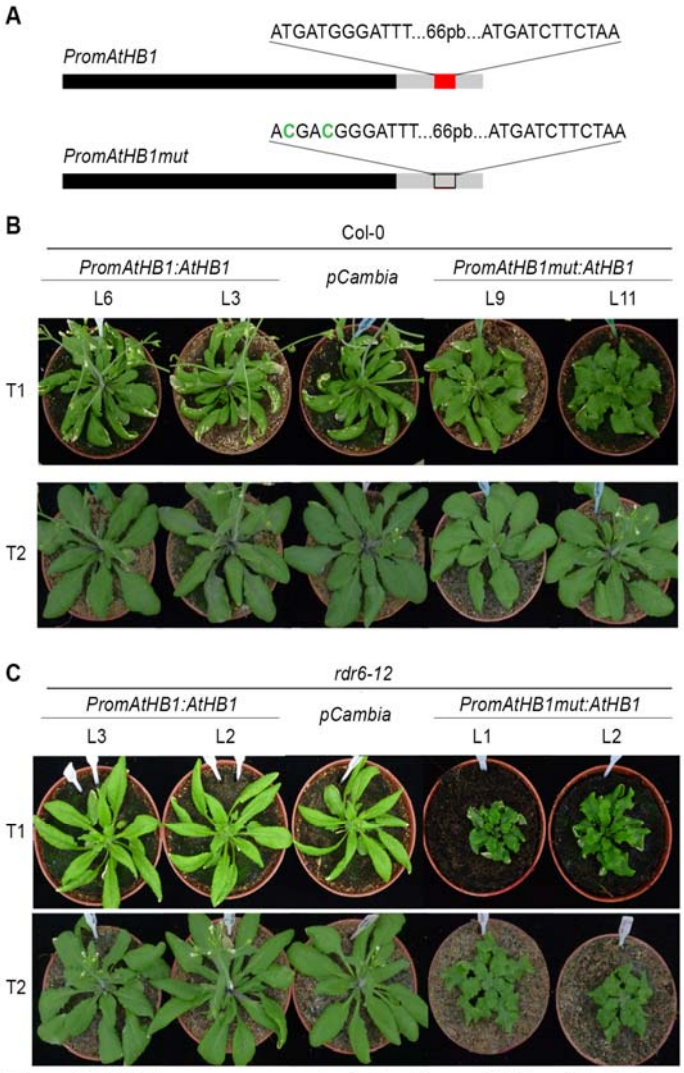

Figure 2. AtHB1 overexpressor plants bearing a uORF mutated in the putative start codons present abnormal phenotypes

A. Schematic representation of the native *AtHB1* promoter (*PromAtHB1*) and a mutated version (*PromAtHB1mut*), both including their 5'UTR. Two single nucleotides, located within the first two codons of the uORF, were mutated (T_C) and are signaled in green.

B. Illustrative photographs of 30-day-old Col-0 plants transformed with *PromAtHB1:AtHB1* and *PromAtHB1mut:AtHB1* compared to control plants transformed with an empty pCambia vector.

C. Illustrative photographs of 30-day-old *rdr6-12* mutant plants transformed with *PromAtHB1:AtHB1* and *PromAtHB1mut:AtHB1* compared to control plants transformed with an empty *pCambia*.

Two independent transgenic lines for each genotype were analyzed. First (T1) and second (T2) generations are shown in the upper and lower panel, respectively.

204 mechanism is only displayed as a result of *AtHB1* overexpression. Considering that the plants

transformed with *PromAtHB1mut:AtHB1* and those transformed with *35S:AtHB1* in the *rdr6-12* background exhibited almost identical phenotypes, it can be concluded that those possessing the mutated version of the uORF are overexpressing *AtHB1*.

CPuORF33 is capable of repressing the translation of different main ORFs

Considering the differential phenotypes showed by *PromAtHB1mut:AtHB1* plants compared to those transformed with the construct bearing the native uORF, we found it reasonable to assume that the uORF is repressing *AtHB1* at the translational level. Supporting this hypothesis, a recent report has shown that CPuORF33 can arrest ribosomes during mRNA translation *in vitro* (Hayashi et al., 2017). Moreover, we did not observe significant differences in *AtHB1* transcript levels between plants transformed with the native or mutated CPuORF33 when the average levels from independent transgenic lines were calculated (Supplemental Figure 4C). Unfortunately, AtHB1 protein levels were not detectable by western blots in Col-0 plants, despite using antibodies against two different tags (HA or His).

Upon discarding CPuORF33 action at the transcriptional level, we decided to perform new genetic constructs in which the expression of the *GUS* reporter gene was driven by the *AtHB1* promoter and the 5'UTR with the native or mutated uORF (*PromAtHB1:GUS* and *PromAtHB1mut:GUS*). Arabidopsis Col-0 and *rdr6-12* plants were transformed with these constructs and several independent single-copy lines were obtained. Considering that the different insertion points for each independent line could lead to different expression levels, lines transformed with each of the constructs and showing similar *GUS* transcript levels (in 14-day-old plants) were selected and taken as pairs. These paired plants were analyzed by histochemistry resulting in the detection of GUS activity in the same tissues (hypocotyls, vascular tissue of the roots and leaves) for both constructs, but with a strong difference in the signal intensity (Figure 3). Plants transformed with *PromAtHB1:GUS* had a weak expression, whereas those transformed with the construct in which the uORF was mutated exhibited a strong GUS color, especially in the leaf lamina (Figures 3B and 3C). Consistent with the observations performed by histochemistry, the quantified GUS enzymatic activity was higher in the extracts obtained from *PromAtHB1mut:GUS* plants than in those from *PromAtHB1:GUS* plants (Figure 3C). These results were independent of the genotype used (Col-0 or *rdr6-12*), indicating the action of a small RNA independent mechanism for translational repression (Supplemental Figure 6).

CPuORF33 represses the translation of the main ORF by a ribosome stalling mechanism

Figure 3

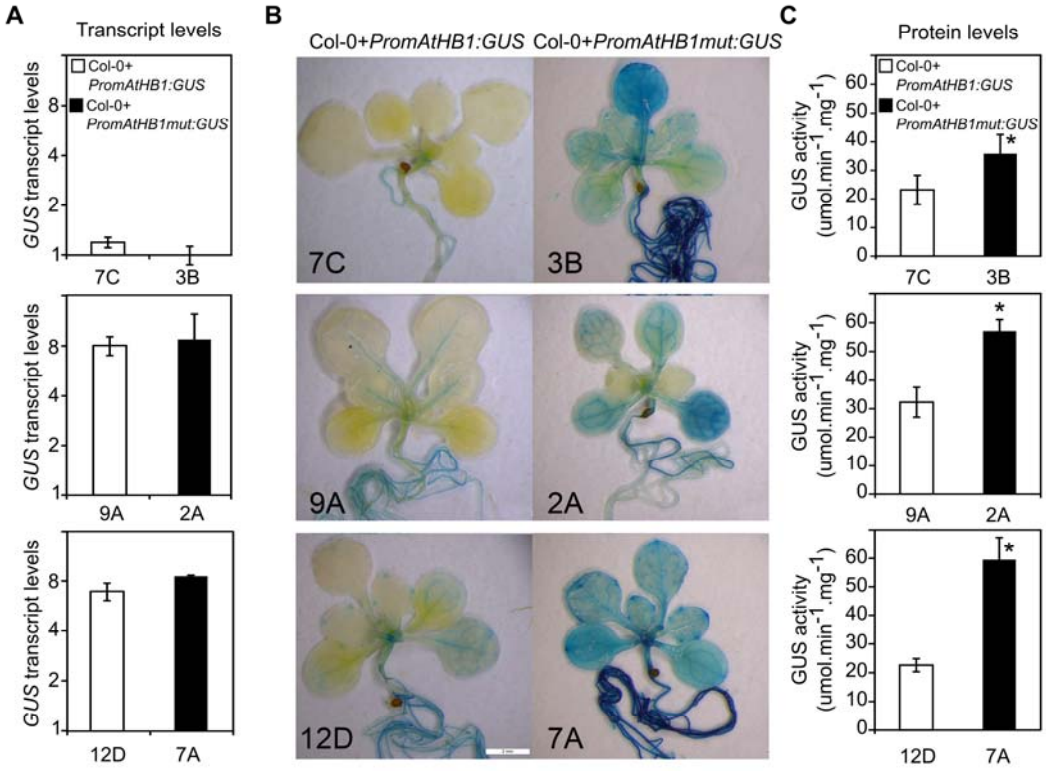

Figure 3. Mutations in the *CPuORF33* enhance the translation of different downstream main ORFs

A. Transcript levels of *GUS* in 14-day-old seedlings of Col-0 plants transformed with native *PromAtHB1:GUS* or *PromAtHB1mut:GUS*. Three independent lines of each genotype are shown, paired according to their transcript levels. Transcript levels in whole rosettes were measured by RT-qPCR and the values were normalized with the smaller absolute value using the ΔΔCt method. Y axis is shown in $\log_2$ scale.

B. *GUS* expression analyzed by histochemical detection of GUS enzymatic activity in 14-day-old plants.

C. GUS activity evaluated by fluorometry in whole rosette protein extracts from the same plants as in A. Error bars: SD of five biological replicates.

T-tests were performed and p-values < 0.05 are signaled with asterisks.

There are several known mechanisms by which uORFs control translation. Among them, NMD (*Nonsense-Mediated Decay*) and ribosome stalling are the most studied. We then considered which mechanism was taking place in the regulation exerted by CPuORF33 on *AtHB1* translation.

In view of the preceding findings, it was unlikely that NMD was taking place. To confirm this and discard the possibility of NMD occurrence, insertional mutant plants of *UPF1* and *UPF3* (*upf1-5* and *upf3-1*, respectively), genes encoding key proteins for NMD, were grown under standard conditions. *AtHB1* transcripts were evaluated in these mutants and the levels were similar to those measured in Col-0 controls (Supplemental Figure 7), indicating that CPuORF33 translational control was not mediated through NMD.

To investigate whether CPuORF33 is capable of acting in *trans* at the transcriptional level, endogenous *AtHB1* transcript levels were assessed in *rdr6-12* mutant plants transformed either with *PromAtHB1:AtHB1* or with *PromAtHB1mut:AtHB1*. To be sure that the quantified transcripts

corresponded to the endogenous *AtHB1*, RT-qPCR assays were performed with primers annealing in the 3'UTR, which is absent in the constructs used to transform these plants. *AtHB1* transcript levels were similar in both genotypes, suggesting that CPuORF33 is not able to act in *trans* at the transcriptional level (Supplemental Figure 8).

Once NMD and *trans*-action were discarded as possible mechanisms exerted by CPuORF33, ribosome stalling was analyzed. Recently, ribosome footprinting analyses with Arabidopsis mRNAs were performed by three different research groups (Juntawong et al., 2014; Merchante et al., 2015, Hsu et al., 2016). These studies permit the identification of transcript regions protected by ribosomes from nucleases action (Ingolia et al., 2009). We used these data to inspect if CPuORF33 is in fact translated and whether it is generating the stalling of the ribosomes. Among these ribosome footprinting experiments, those described by Juntawong et al. (2014) and Hsu et al. (2016) were the most informative for the case of *AtHB1*. These authors used seedlings grown under long-day regimes, similar experimental conditions to those used in our experiments, whereas Merchante et al. (2015) used etiolated seedlings.

The analyses of the data are shown in Supplemental Figure 9. The results indicated that the uORF had a higher occupation density compared to other 5'UTR regions and to the mORF. Weak peaks upstream from the CPuORF33 were also detected and, considering the absence of AUGs in this region, they indicated that uORFs starting at non-AUG codons (Laing et al., 2015) should not be discarded. However, the differences in translation efficiency would suggest that their relative importance with respect to CPuORF33 is much lower.

Furthermore, the CPuORF33 did not exhibit a normal distribution but presented a peak at the end of the uORF, suggesting ribosome stalling. It is important to note that three different experiments resulted in similar results, showing clearly different ribosome footprinting profiles when compared to that of AtHB13, another TF from the same HD-Zip I family (Supplemental Figure 9). A ribosome stalling process implies the interaction between the nascent peptide and the ribosome. Hence, we decided to test the importance of the CPuORF33 amino acid sequence by generating an additional genetic construct in which the frame of the uORF was shifted. In order to make the analysis independent of the transcriptional activity of *AtHB1* promoter, the native or mutated 5'UTR of *AtHB1* were cloned downstream of the *35S CaMV* constitutive promoter driving the expression of the *GUS* reporter gene (*35S:native-uORF:GUS* and *35S:FS-uORF:GUS*, respectively). A schematic representation of these constructs is shown in Figure 4A. In the *35S:FS-uORF:GUS* construct, the nucleotide sequence exhibits minimal changes, whereas the amino acid sequence is completely altered. Col-0 plants were transformed using these genetic constructs and the *GUS* expression pattern

Figure 4

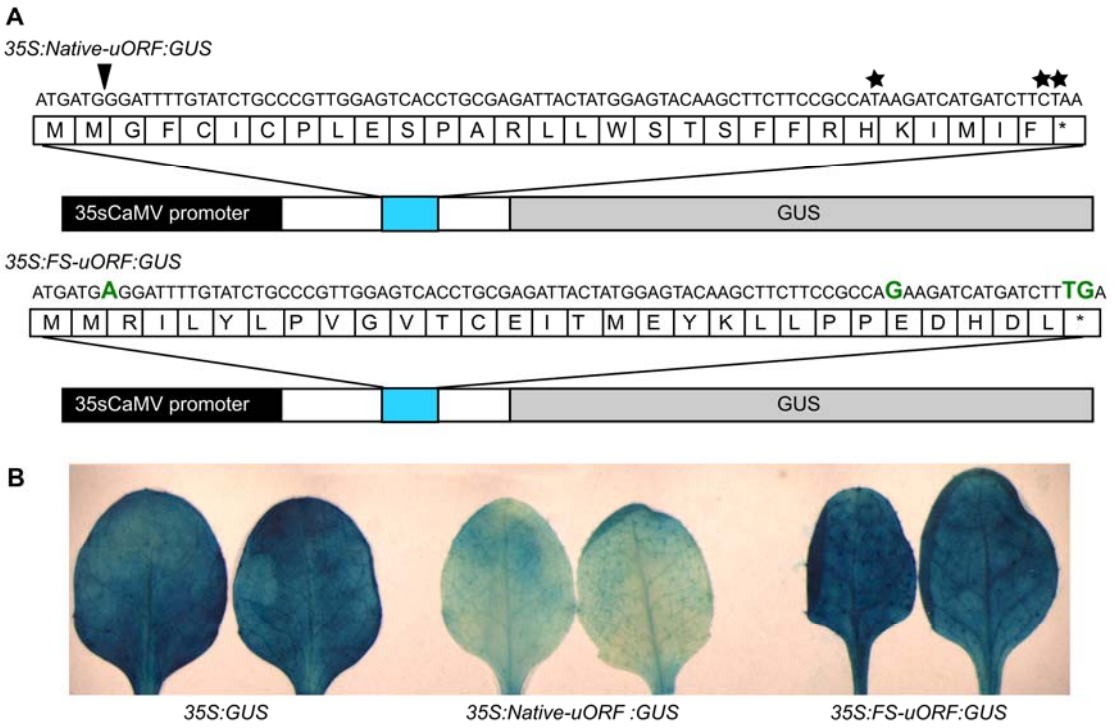

Figure 4. Ribosome footprinting pattern and mutations in the uORF amino acid sequence suggest ribosome stalling at the CPuORF33

A. Schematic representation of the constructs used in Arabidopsis transformation, showing the nucleotide (above) and amino acid (below) sequence of the native and mutated uORF. *FS*: Frame shift. *Black*: *35SCaMV promoter*, *White*: *AtHB1 5'UTR*, Light blue: *CPuORF33*, Grey: *GUS ORF*. *Stars*: Single base modification, *Arrow*: Insertion introduced.

B. Illustrative photograph of 20-day-old leaves transformed with the indicated constructs and analyzed by GUS histochemisty.

analyzed by histochemistry. As shown in Figure 4B, the uORF with the shifted frame was unable to repress *GUS* expression.

To further test the importance of the amino acid sequence, different mutations were generated in the uORF sequence. They were cloned upstream from the GFP mORF and yeast cells were transformed with these constructs. Protein extracts were analyzed by western blots indicating reduced levels of GFP when the native uORF was used (Supplemental Figure 10). In contrast, no repression was observed when the amino acid sequence of the uORF was significantly altered (from residues 3 to 25 or 3 to 29). Interestingly, changes on the N-terminal of the CPuORF33 partially repressed GFP levels, indicating that certain amino acids are more important than others for translational repression (Supplemental Figure 10). Altogether, these results supported the ribosome stalling mechanism and its dependence on the amino acid sequence encoded by the uORF.

The activity of CPuORF33 is tissue-specific

In view of the described observations, we wondered whether CPuORF33 activity depended on the tissue, developmental stage or growth condition. To address this question, Col-0 plants transformed with *35S:native-uORF:GUS* or *35S:GUS* were analyzed in detail by histochemistry (Figure 5A). Cotyledons of five-day-old seedlings, fully developed leaves and inflorescences of plants transformed with *35S:native-uORF:GUS,* grown under a long-day photoperiod, clearly showed CPuORF33 repression (Figure 5). However, leaf primordia and roots of the same plants exhibited the same GUS staining as those transformed with *35S:GUS*. The observations indicated that the action exerted by CPuORF33 was tissue-specific. Similar results were obtained when plants transformed with *35S:native-uORF:GUS* were compared with plants transformed with *35S:FS-uORF:GUS* (data not shown). RiboSeq assays performed in roots and aerial tissue by Hsu et al. (2016) were consistent with our observations (Supplemental Figure 11).

This phenomenon could be the result of an alternative splicing event or the presence of a secondary transcription start site (TSS) that prevents the inclusion of the complete CPuORF in the mature mRNA. Indeed, the inspection of publicly available TSS results from whole *A. thaliana* roots using the PEAT (Paired-End Analysis of Transcription start sites) protocol indicated that the *AtHB1* locus presented a second TSS with a "weak peak" pattern between locus positions 194 and 403 (Peak_40644; Supplemental Figure 12A; Morton et al., 2014). This TSS would exclude from the mRNA the CPuORF start codon, which is at position 163. To further investigate this hypothesis, we used published RNA-Seq data to compare the mRNA profiles between shoots and roots and found no strong indication of alternative splicing and disparate results for a secondary TSS (Supplemental Figure 12B-E). To test the secondary TSS hypothesis in our conditions, the tissue differential presence of a shorter *AtHB1* transcript excluding the CPuORF start codon was tested by RT-qPCR in roots and shoots using two sets of oligonucleotides (Supplemental Figure 12A). A within-tissue ratio of amplification products was calculated and compared between shoots and roots; but results indicated no significant differences (data not shown). In consequence, although there is some evidence supporting the existence of a secondary TSS, this would not be the key mechanism explaining the tissue-specificity observed for the activity of the CPuORF.

CPuORF33 repression activity is triggered by light in aerial tissues

As mentioned above, CPuORF33 was active in aerial tissues and inactive in roots (Figure 5). Thus, an attractive hypothesis was that CPuORF action could be triggered somehow by light. In order to test this, *35S:native-uORF:GUS* transformed plants were grown during six days in complete darkness or under the long-day photoperiod (LDP) and GUS activity was evaluated by histochemistry. As shown in Figure 6A, cotyledons of seedlings grown in darkness were completely

Figure 5

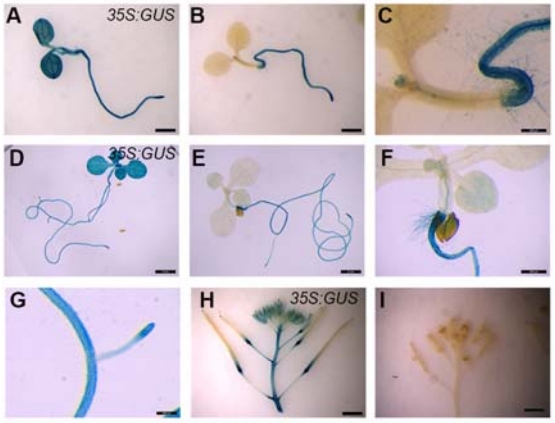

Figure 5. CPuORF33 repression action depends on the tissue and environmental condition
Illustrative photographs of organs/tissues of plants revealed by GUS histochemisty. **A**. 5-day-old seedling transformed with *35S:GUS* grown under long day photoperiod (LDP). Bar: 2 mm; **B.** 5-day-old seedling transformed with *35S:native-uORF:GUS* grown under LDP. Bar: 2 mm; **C.** hypocotyl detail of B. Bar: 500 µm; **D.** 10-day-old seedling transformed with *35S:GUS* grown under LDP. Bar: 2 mm; **E.** 10-day-old seedling transformed with *35S:native-uORF:GUS* grown under LDP. Bar: 2 mm; **F.** hypocotyl detail of E. Bar: 500 µm; **G.** root detail of E. Bar: 200 µm; **H.** inflorescence of plants transformed with 35S:GUS. Bar: 5 mm; **I.** inflorescence of plants transformed with *35S:native-uORF:GUS*. Bar: 5 mm.

stained, indicating a lack of uORF repression under this condition, whereas the opposite scenario was obtained under LDP. Moreover, the effect of illumination was not reverted in these plants after two days of darkness (Figure 6B). Similar results were obtained using 15-day-old plants placed in darkness for five additional days (Supplemental Figure 13).

To determine whether CPuORF33 repression activity was the result of the illumination quality, 6-day-old seedlings transformed with *35S:native-uORF:GUS* were grown under LDP exposed to blue, red or white light. All these treatments resulted in similar observations, i.e. CPuORF33 actively repressed GUS activity in aerial tissues (Supplemental Figure 13). Additional treatments with ABA, IAA and gibberellins were also carried out on dark-grown seedlings, indicating that none of these hormones were able to modify CPuORF33 repression (data not shown). Considering the hypothesis of a chloroplast signal as the switch to activate CPuORF33, *35S:native-uORF:GUS* seedlings grown in complete darkness over six days were treated with DCMU (dichlorophenyl dimethylurea) and transferred to light conditions for an additional 24 h. Notably, the repression action of CPuORF33 was avoided as GUS activity was clearly detected in cotyledons (Figure 6C), indicating that a signal from coupled chloroplasts is responsible for initiating CPuORF33 activity.

The homologous maize CPuORF also functions as a translational repressor

Figure 6

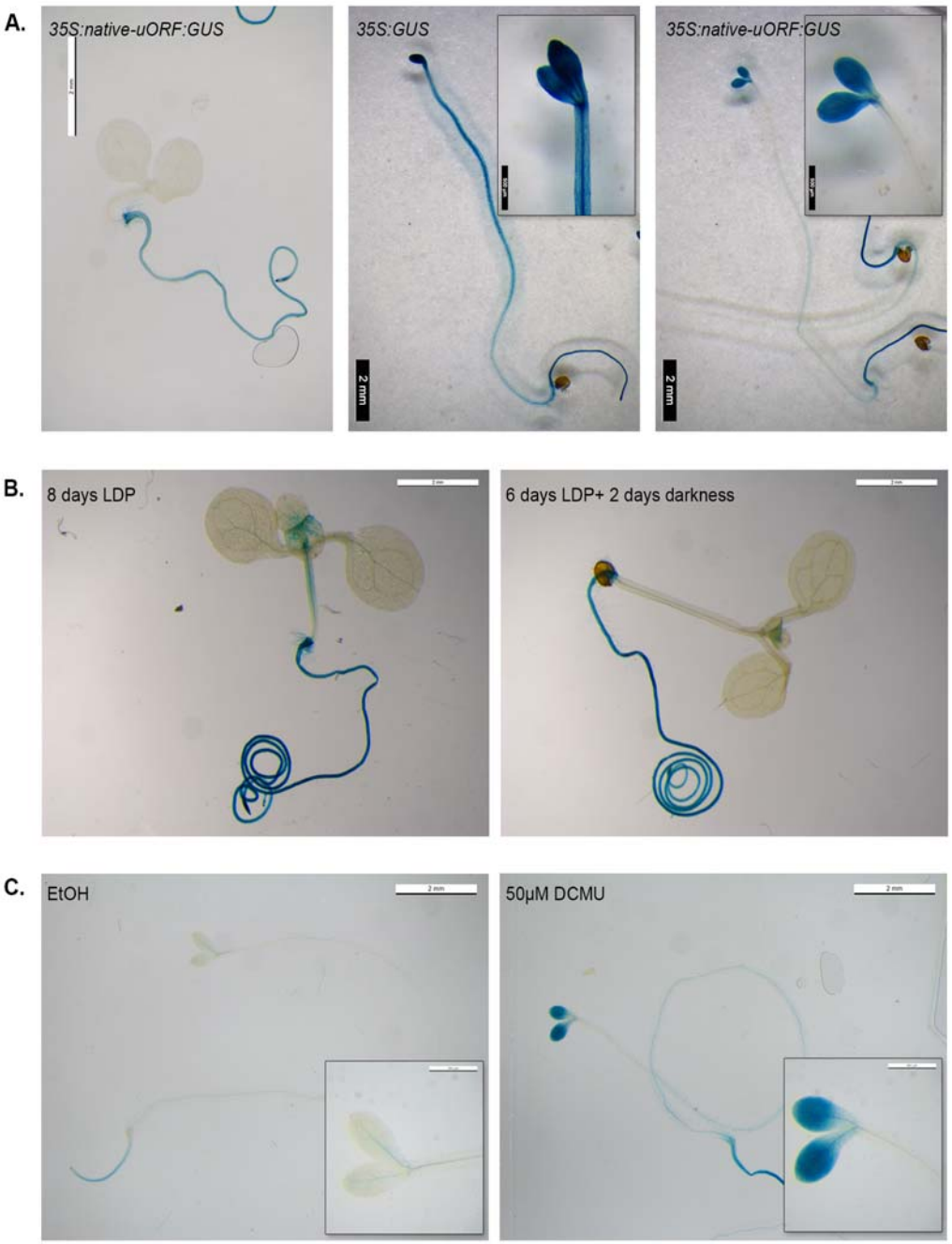

Figure 6. Light-dependent CPuORF33 repression action in cotylendons is not reverted in darkness but avoided by DCMU

Illustrative photographs of seedlings transformed with *35S:GUS* or *35S:native-uORF:GUS* and revealed by GUS histochemisty. **A:** *Left*: 6-day-old seedling transformed with *35S:native-uORF:GUS* grown under long day photoperiod (LDP) *Center*: 6-day-old seedling transformed with *35S:GUS* grown in darkness. *Right*: 6-day-old seedling transformed with *35S:native-uORF:GUS* grown in darkness. Bar: 2 mm; **B:** *Left*: 8-day-old *35S:native-uORF:GUS* seedlings grown under LDP. *Right*: 6-day-old 35S:native-uORF:GUS seedlings grown under LFP and then transferred for 2 additional days to darkness. Bar: 2 mm; **C:** *Left*: 6-day-old *35S:native-uORF:GUS* seedlings grown in darkness and treated with ethanol during 24 h with ethanol under LFP. *Right*: 6-day-old *35S:native-uORF:GUS* seedlings grown in darkness and treated during 24 h with 50 µM DCMU under LFP. Bar: 2 mm.

347 Monocot plants exhibit an insertion of seven amino acids in the carboxy-termini of the CPuORF,

Figure 7

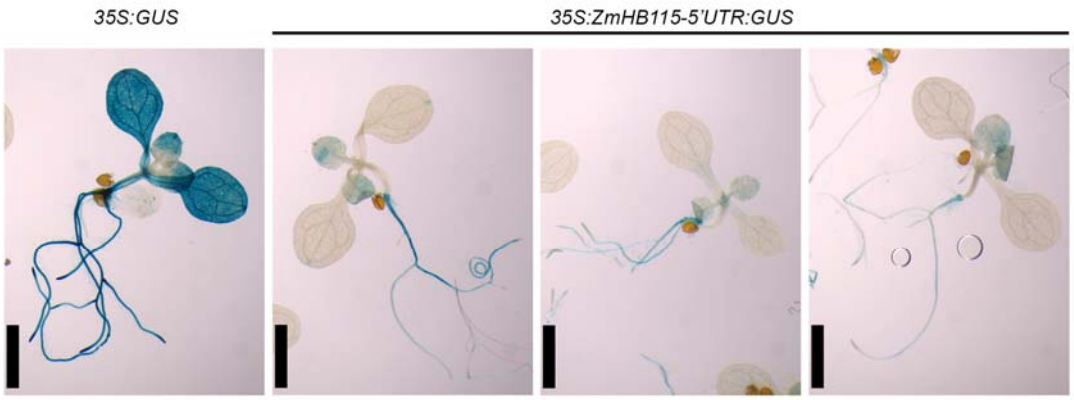

Figure 7. The uORF of maize AtHB1' homolog functions as a translational repressor

Illustrative photographs of 14-day old plants revealed by GUS histochemisty. Left photograph: Arabidopsis plants transformed with *35S:GUS* grown under long photoperiod. Right photographs: three independent lines of Arabidopsis plants transformed with *35S:maize5'UTR:GUS* grown under long photoperiod. Bar: 500 µm

348 which makes them longer than those of dicot plants (Figure 1A). To evaluate whether this longer
349 peptide resulted in a different function, we decided to clone a monocot uORF and analyze its
350 activity. To this end, the maize 5'UTR region of the *AtHB1* homolog (*ZmHB115*) was cloned
351 between the constitutive *35S CaMV* promoter and the *GUS* reporter gene. Arabidopsis plants were
352 then transformed and analyzed by GUS histochemistry (Figure 7A). The results indicated that the
353 maize uORF represses GUS translation in the aerial portions of the plant, similar to the inhibition
354 seen for the Arabidopsis CPuORF33. Notably, as its Arabidopsis homolog, the maize uORF also
355 exhibited tissue-specific activity and did not function as a repressor in roots (Figure 7A).
356 Aiming to elucidate if this uORF is active in maize, data obtained from ribosome footprinting
357 analyses performed with samples of 14-day-old maize seedlings were examined (Supplemental
358 Figure 14; Lei et al., 2015). As expected, translation seemed to be stalled in the uORF region and
359 less ribosomes were detected in the mORF (Supplemental Figure 14), supporting both the proposed
360 ribosome stalling mechanism and the conservation between species of the uORF´s function.
361
362 <u>The absence of a tightly regulated expression of *AtHB1* causes severe deleterious effects</u>
363 It was surprising to discover such a sophisticated mechanism repressing *AtHB1* expression,
364 especially because we were not able to detect strong differential phenotypes in *athb1* mutants and
365 certainly no lethality in Col-0 plants transformed with *35S:AtHB1* (Capella et al., 2015b).
366 To understand such phenomena, we decided to further analyze *rdr6-12* plants transformed with
367 *PromAtHB1mut:AtHB1* in which neither ribosome stalling nor small RNA silencing were possible.
368 As controls, we used *rdr6-12* plants transformed with an empty vector or with *PromAtHB1:AtHB1*.

Hypocotyl length was analyzed in these plants since this developmental trait is affected by AtHB1 (Capella et al., 2015b). As expected, *rdr6-12* plants transformed with *PromAtHB1mut:AtHB1* showed longer hypocotyls than the other transformed plants (Figure 8A). In parallel, plants from the three genotypes were grown on soil under standard conditions. *PromAtHB1mut:AtHB1* plants exhibited compact rosettes, a delay in bolting and more importantly, a strongly altered flower morphology. Pistils were reduced, anthers were extremely short and non-dehiscent, and siliques were small and had fewer or no seeds. In several lines, the analysis of a second generation was not possible because T1 plants were sterile (Figure 8B). Altogether, these results could explain why such a sophisticated mechanism is acting to repress overexpression of this TF, i.e. unregulated increased expression of *AtHB1* conducted to an infertile, delayed and aberrant phenotype.

Figure 8

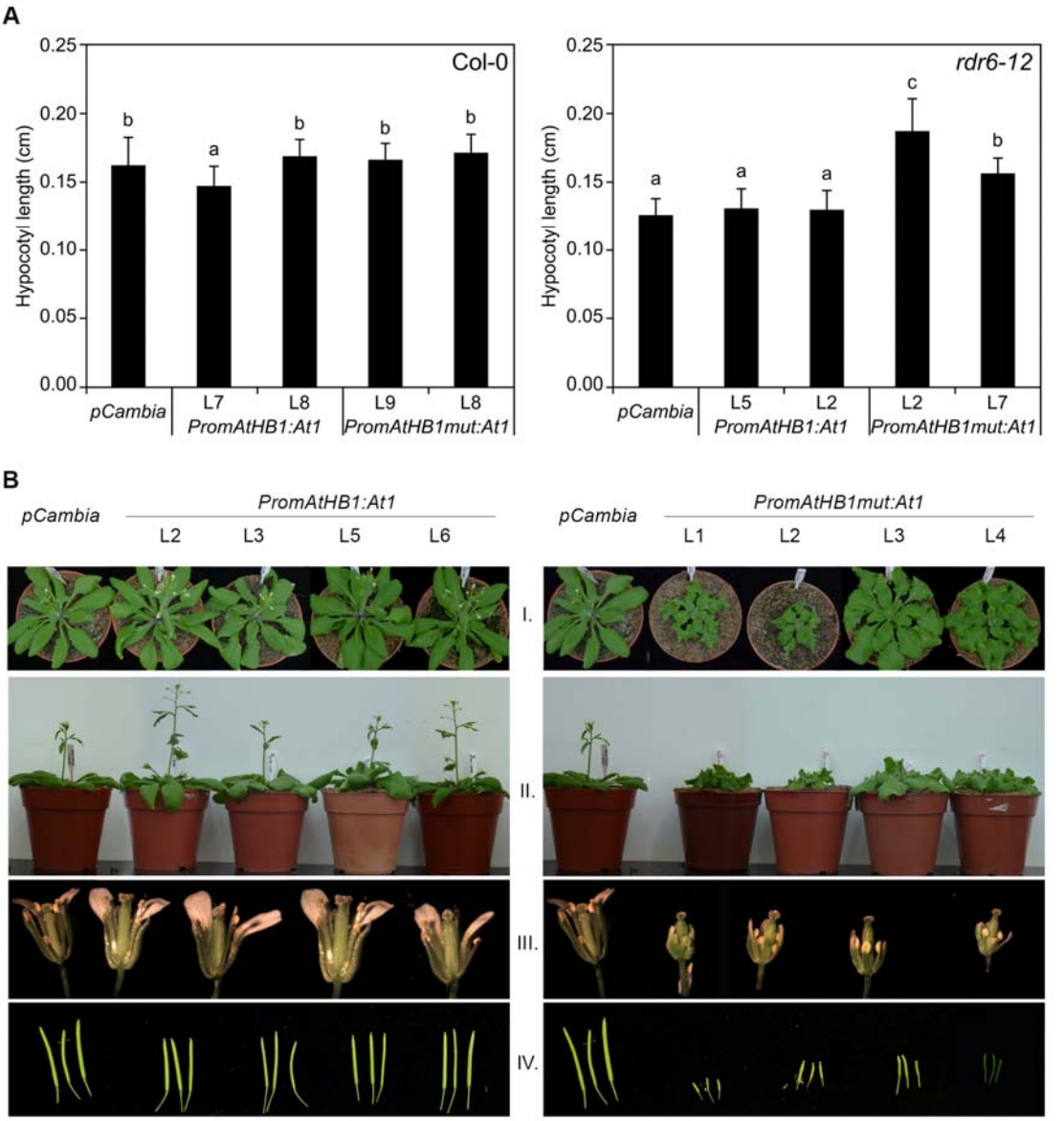

Figure 8. Expression levels of *AtHB1* are fine-tuned due to the detrimental effects for plant reproduction and survival generated by its overexpression

A. Hypocotyl length of plants grown under short photoperiod for 5 days. Control plants of Col-0 and *rdr6-12* backgrounds are shown as well as the same plants transformed with *PromAtHB1:AtHB1* (*PromAtHB1:At1*) and *PromAtHB1mut:AtHB1* (*PromAtHB1mut:At1*). Two independent lines for each genotype are shown. An ANOVA test was performed and pair-wise differences were evaluated with a Tukey *post hoc* test; different groups were marked with letters at 0.05 significance level.

B. Illustrative photographs of rdr6-12 plants transformed with *PromAtHB1:AtHB1* and *PromAtHB1mut:AtHB1*. I. 25-day-old rosette leaves of control and transformed plants. Four independent lines are shown for each genotype. II. Front photograph of the same plants as in I. III. Flowers of 40-day-old plants. IV. Siliques of the same plants.

384

Discussion

The adaptation of plants throughout evolution involved the loss and the acquisition of genome DNA sequences including the conservation of key elements. Many of such conserved regulatory elements must be fundamental for plant development, reproduction and/or survival. Here we demonstrated that a highly conserved genetic element, the CPuORF33, is important to avoid plant sterility.

Although uORFs are present in a considerable number of mRNAs (Hayden et al., 2008; Nagalakshmi et al., 2008; Calvo et al., 2009), it is remarkable that only a small portion of these varied genetic elements has been conserved between species, and only a few members within this group were assigned a function. Here we show that CPuORF33 negatively regulates *AtHB1* translation during plant development and this regulatory mechanism is conserved in maize. Hence, it is tempting to suggest that a similar scenario occurs in other species with *AtHB1* homologs. Notably, in all the available DNA sequences encoding *AtHB1* homologs that have known 5'UTRs, either from monocot or dicot species, CPuORF33 was identified. Considering that the number of sequences continuously increases, it would be interesting to repeat this analysis in the near future.

Besides the high conservation of the nucleotide sequence, it is important to note that the amino acid sequence is even more conserved, indicating that the peptide, and not the RNA, is the active element. This suggestion was also supported by the absence of overlap between CPuORF33 and the main ORF. This characteristic is relevant to allow ribosome reinitiation and the translation of the mORF. Overlap of the CPuORF and the mORF was described as being linked to NMD regulating the abundance of many gene transcripts involved in plant development, including TFs, RNA processing factors and stress response genes (Kalyna et al., 2011).

According to previous reports, the regulation exerted by eukaryotic uORFs on transcript levels of the main ORF occurs through several different mechanisms of action, but most uORFs exert their effects in a sequence-independent manner (Calvo et al., 2009). In contrast, certain uORFs control translation of the mORF in a peptide sequence-dependent manner (Ito et al., 2013; von Armin et al., 2014). Among the possible repression mechanisms exerted by uORFs, NMD is the one acting in the regulation of *AdoMetDC1,* which causes polyamine-responsive ribosomal arrest, the *SAC51* gene encoding a bHLH transcription factor, and *AtMHX*, which encodes a vacuolar magnesium-zinc/proton exchanger (Bender and Fink, 1998; Imai et al., 2006; Combier et al., 2008; Saul et al., 2009; Uchiyama-Kadokura et al., 2014). On the other hand, other mechanisms displayed by uORFs regulate RNA translation; among them are ribosome stalling (Rahmani et al., 2009; Alatorre-Cobos et al., 2012; Wiese et al., 2004), ribosome reinitiation (Wang and Wessler, 1998), a combination of both (Hanfrey et al., 2005) and others not well understood (Kwak and Lee, 2001). Among the

possible mechanisms of CPuORF33 action, we were able to show that this particular element repressed *AtHB1* translation in *cis*.

During translation, ribosome movement along the mRNA molecule can be stopped either by a stable secondary structure in the mRNA or by the nascent translated peptide. Both cases can be observed in ribosome footprinting experiments as an evident increase in the number of reads in a particular region. The ribosome footprinting analyses for the 5'UTR region of *AtHB1* showed a clear coverage peak ~40 bp upstream of the uORF stop codon, suggesting the stalling of ribosomes in this region. This peak should not be confused with the one caused by the deceleration of ribosome movement during translational termination, which appears ~16 pb upstream of the stop codon (Juntawong et al., 2014; Hou et al., 2016). Taking into account the high conservation observed in the amino acid sequences of CPuORF33 homologs, not so evident at the nucleotide level, it is tempting to speculate that the ribosome stalling is caused by the nascent peptide and not by a secondary structure in the mRNA. Supporting this conclusion, the repressive activity of the uORF is lost when frame shift mutations were introduced, in both plants and yeast, even though there are only minor changes in the RNA sequence.

In this work we demonstrated the importance of the peptide structure of the CPuORF33 for *in vivo* translational repression, most likely by ribosome stalling. In this mechanism, the interaction between the polypeptide being synthesized and the ribosome tunnel can regulate translation rate. The tunnel allows the formation of secondary structures like α-helix or Zinc finger motifs (Nilsson et al., 2015). A recent report by Ebina and coworkers (2015) identified 16 novel uORFs in which the amino acids located at the carboxy-termini were crucial in determining their repressive action. In order to test the functionality of the CPuORF33 carboxy terminus, its peptide sequence was changed by two point mutations; one located at amino acid 24 (H→Q) and the second one deleting the stop codon, which adds 30 additional amino acids (*mut5'UTR*). However, no differences were observed in plants transformed with *35S:mut5'UTR:GUS* compared to those transformed with the native 5'UTR (data not shown). This indicates that CPuORF33 is more likely a class II uORF in which, according to Takahashi et al. (2012), the carboxy-terminal is not relevant for its action.

In contrast with our results, using an *in vitro* system Hayashi et al. (2017) showed that CPuORF33 (called At3g01470 by the authors) arrests ribosomes in a peptide sequence-independent manner. A plausible explanation for this discrepancy could be that the sequence-dependent ribosome arrest activity needs a certain biomolecule to be absent in the *in vitro* system. An alternative explanation could be that, as in the *in vitro* assay, an N-terminal GST fusion protein was used, such that the 3D structure of the CPuORF33 could have been affected.

There are some reports showing that the ribosome stalling mechanism involves small molecules like ascorbate, boron (as H_3BO_3 in solution), phosphocholine or sucrose (Rahmani et al., 2009; Alatorre-Cobos et al., 2012; Laing et al., 2016; Tanaka et al., 2016). Further studies will be necessary to reveal whether those or other molecules are necessary for CPuORF33 action. Nonetheless, even when unidentified molecules were necessary for *AtHB1* repression, such molecules are normally present in plant leaves and flowers since we observed the repression exerted by CPuORF33 in these tissues, especially when using stably transformed plants with the *35S:native-uORF:GUS* and *35S:FS-uORF:GUS* constructs, which make the analysis independent of transcriptional regulation. Moreover and in view of the tissue specific action of CPuORF33, one could speculate that such molecules, that could also be proteins, are not present in roots and apical meristems.

Considering the differences between the roots and aerial parts of the plant, and also those between darkness and light, chloroplast functionality was assessed for its capacity to regulate CPuORF33 using DCMU (a known photosynthesis uncoupler). This treatment was able to inhibit CPuORF repressor action (Figure 6). Additionally, several molecules related to photosynthesis, including sugars and hormones, were tested with negative results. Further investigation will be needed to reveal which is the chloroplast signal responsible for this effect.

Another mechanism which might be potentially responsible for the tissue-specific action of CPuORF33 was considered. A secondary transcription start site in *AtHB1* was found by Morton et al. (2014) and was defined as a region located downstream of the uORF start codon (Supplemental Figure 12A). Transcripts starting at this region would therefore lack the full uORF, preventing the stalling of ribosomes and allowing the uninhibited expression of the mORF. However, the comparison of RNA transcript profiles between roots and shoots using publicly available data was not conclusive and our qPCR assays comparing these tissues did not support this mechanism. In consequence, the presence of a secondary TSS would not be able to explain the tissue-specificity of uORF activity. Nonetheless, we cannot rule out that this TSS could be functional in bypassing the repressive action of the uORF under certain conditions, as reported for other uORFs (Pumplin et al., 2016).

The second mechanism repressing *AtHB1* expression described in this work is mediated by small RNAs, although this might only function when it is expressed as a transgene. It is already known that above a certain threshold, the expression of several transgenes like *GUS*, *GFP* or *SPT* (*Streptomycin Phosphotransferase*) is silenced by such a mechanism, being threshold dependent on the gene (Schubert et al., 2004; Rajeevkumar et al., 2015). Two different mechanisms acting to silence transgenes have been described: the TGS (Transcriptional Gene Silencing) and the PTGS (Post-Transcriptional Gene Silencing). In the first one, a DNA segment encoding a certain mRNA is

methylated inhibiting transcription, whereas in the second the mRNA is degraded by siRNA after the formation of the mRNA (Matzke et al., 2001). PTGS occurs during plant development and after meiosis initiation, whereas TGS occurs during meiosis and is heritable (Vaucheret and Fagard, 2001). Since the repression of *AtHB1* in transgenic plants takes place in the second generation, TGS is likely the silencing mechanism. However, it is rather infrequent that such silencing was displayed when the overexpression is controlled by a native promoter since this scenario has been observed only with constitutive promoters like the *35S CaMV*. These observations indicate that *AtHB1* overexpression is tightly regulated to avoid expression above the threshold and that this threshold is very close to endogenous transcript levels. Moreover, *AtHB1* was not silenced when the construct used to perform the transformation did not have the *AtHB1* CDS (not shown), indicating that the silencing is caused by *AtHB1* transcript or protein levels but not by the promoter itself.

We can conclude that the CPuORF33 present in the 5' untranslated region of the Arabidopsis homeodomain-leucine zipper transcription factor AtHB1 and its homologs in at least other 43 species exerts a strong tissue and condition specific regulation at the translational level by ribosome stalling in order to avoid an aberrant phenotype.

Materials and methods

Plant material and growth conditions

Arabidopsis plants were grown directly on soil in a growth chamber at 22–24 °C under long-day photoperiod (16 h light), at an intensity of approximately 120 μmol m^{-2} s^{-1}, in 8 x 7 cm pots. Short photoperiod conditions were used only to evaluate hypocotyl length as indicated in the corresponding figure legend.

Arabidopsis thaliana ecotype Columbia (Col-0), and the mutants *athb1-1* (SALK_123216C), *upf3-1* (SALK_025175) and *upf1-5* (SALK_112922), all in the Col-0 ecotype background, were obtained from the Arabidopsis Biological Resource Center (ABRC, http://www.arabidopsis.org; Columbus, OH, USA). The mutant seeds *rdr6-12* (Peragine et al., 2004) were kindly provided by Dr. Pablo Manavella from the Instituto de Agrobiotecnología del Litoral, Santa Fe, Argentina. *pKGWFS7 PromAtHB1:GUS* plants were previously described (Capella et al., 2015b). Homozygous lines were selected after two complete growth cycles.

DCMU treatments

Seeds were surface sterilized and then plated in Petri dishes with 0.5 x Murashige and Skoog medium supplemented with vitamins (MS, PhytoTechnology LaboratoriesTM). Plates were placed at 4 °C during 2 days and transferred to the growth chamber (22–24 °C under long-day photoperiod) for the periods indicated in the corresponding figure legends. Another group of plates was transferred to the same chamber but inside a dark box. For DCMU treatments, these plants were vacuum-infiltrated with 50 μM DCMU solution; then, the liquid reagent was discarded and plants were placed under long-day photoperiod under light for additional 24 h.

Genetic constructs

pCambia HA-AtHB1 was previously described (Capella et al., 2015b).

PromAtHB1mut:GUS: This construct was carried out by PCR amplification and overlapping with the oligonucleotides (Higuchi et al., 1988) listed in the Supplemental Table S2 using as probe the *pKGWFS7 PromAtHB1:GUS* construct. The amplification PCR product was cloned in *pBluescript SK-*. This last construct was restricted with *Bgl*II and *Hind*III and finally inserted in *pKGWFS7 PromAtHB1:GUS*, replacing the wild-type sequence. The correct insertion was verified by sequencing.

PromAtHB1:AtHB1* and *PromAtHB1mut:AtHB1: The native and mutated versions of *AtHB1* promoter were amplified using specific oligonucleotides (Supplemental Table S2) and *pKGWFS7*

PromAtHB1:GUS and *pKGWFS7 PromAtHB1mut:GUS* as templates, respectively. The PCR products were cloned into the *Sal*I and *Xba*I sites of *pMTL22*, and then the obtained clones were digested with *Bam*HI and *Xba*I. Finally, these products were cloned into the *Bgl*II and *Xba*I sites of *pCambia HA-AtHB1*, replacing the 35S cauliflower mosaic virus (CaMV).

35S:native-uORF:GUS: The *AtHB1* 5'UTR was amplified by PCR using as template the *pCambia PromAtHB1:AtHB1* clone and specific oligonucleotides (Supplemental Table S2). The amplification product was then cloned into the *Xba*I and *Bam*HI sites of *pBI121*.

35S:FS-uORF:GUS: The indicated mutations were introduced by PCR amplification and overlapping with the oligonucleotides listed in the Supplemental Table S2 and using as probe the *pCambia PromAtHB1:At1* clone. The PCR product was cloned into the *Xba*I and *Bam*HI sites of *pBI121*.

35S:ZmHB115-5'UTR:GUS: The *ZmHB115* 5'UTR was amplified by PCR using genomic DNA as template and specific oligonucleotides (Supplemental Table S2). The amplification product was then cloned into the *Xba*I and *Bam*HI sites of *pBI121*.

pADH::yeGFP and ***pADH::NLS::yeGFP***: The yeast enhanced GFP (yeGFP), with or without the SV40 NLS, was amplified by PCR using as template the *pYM25* vector and specific oligonucleotides (Supplemental Table S2). The amplification products were then cloned into the *Bam*HI and *Sal*I sites of *YCplac22 pADH*.

pADH::uORF::yeGFP and ***pADH::FS-uORF::yeGFP*** mutant constructs: *native-uORF* and *FS-uORF* were amplified using specific oligonucleotides (Supplemental Table S2) and the *35S:native-uORF:GUS* and *35S:FS-uORF:GUS* clones as probes. By Gibson cloning (NEB), the PCR products were clone into *pADH::yeGFP*, previously restricted with *Bam*HI. Finally, the indicated mutations (FS1, FS2 and FS3) were introduced by QuikChange II Site-Directed Mutagenesis (Agilent), using *pADH::FS-uORF::yeGFP* as template.

Stable Arabidopsis plants transformation

Transformed *Agrobacterium tumefaciens* strain LBA4404 was used to obtain transgenic Arabidopsis plants by the floral dip procedure (Clough and Bent, 1998). Transformed plants were selected on the basis of their specific resistance in Petri dishes with 0.5 x Murashige and Skoog medium supplemented with vitamins (MS, PhytoTechnology LaboratoriesTM) and the appropriate selector chemical (kanamycin 50 mg/l or hygromycin 25 mg/l). The seeds were surface sterilized, plated and after 2 days of incubation at 4 °C placed in a growth chamber at 22–24 °C.

The insertion of each transgene was checked by PCR using genomic DNA as template with specific oligonucleotides listed in Supplemental Table S2. Three/four positive independent lines for each

construct were further reproduced and homozygous T3 and T4 plants were used in order to analyze expression levels of the specific transgene and plants phenotypes. T1 plants were used in a specific experiment as indicated in the corresponding figure legend.

RNA extraction and analysis

Total RNA for transcript levels evaluation by RT-qPCR was isolated from Arabidopsis leaves using the Trizol® reagent (Invitrogen) according to the manufacturer's instructions. One µg of RNA was reverse-transcribed using oligo$(dT)_{18}$ and M-MLV reverse transcriptase II (Promega). For alternative TSS assay, a different oligonucleotide (AtHB1qPCRR) was used for reverse transcription. Quantitative real-time PCR (qPCR) was performed with the Mx3000P Multiplex qPCR system (Stratagene, La Jolla, CA) in a 20 µl final volume containing 2 µl SyBr green (4 x), 8 pmol of each primer, 2 mM $MgCl_2$, 10 µl of a 1/15 dilution of the RT reaction and 0.1 µl Taq Platinum (Invitrogen). Fluorescence was measured at 72 °C during 40 cycles. Specific primers were designed (Table S3). Quantification of mRNA levels was performed by normalization with the *Actin* transcripts levels (*ACTIN2* and *ACTIN8*) according to the ΔΔCt method (Pfaffl, 2001). All the reactions were performed with, at least, three replicates. For a better visualization of the results, the y axes of the figures containing transcripts evaluation were represented in a logarithmic scale.

Histochemical GUS staining

GUS staining was performed as described by Jefferson et al. (1987). Plants were immersed in GUS staining buffer (1 mM 5-bromo-4-chloro-3-indolyl-glucuronic acid in 100 mM sodium phosphate pH 7.0, 0.1 % Triton X-100, 100 mM potassium ferrocyanide), vacuum was applied for 5 min, and then plants were incubated at 37 °C for 12 h. Chlorophyll was cleared from the plant tissues by immersion in 70 % ethanol.

Phenotype analyses

Plants were grown as described above and photographed using a Panasonic DMC-FH4 camera. Flowers and siliques were detached and photographed under a stereomicroscope Nikon SMZ800. Hypocotyl length measurements were carried out as described (Capella et al., 2015b).

In-silico sequence analysis

To retrieve nucleotide sequences, initially a BLASTP search was conducted with the full-length sequence of AtHB1 transcription factor against the NCBI non-redundant protein sequence database (default parameters were used, January 18, 2016; Altschul et al., 1990). Sequence redundancy was

checked using the "skipredundant" program of the EMBOSS package (Rice et al., 2000) and the results were manually inspected and curated. After this filtering, full mRNA-containing hits were selected for further analysis.

The amino acid sequence of CPuORF33 was analyzed for the prediction of secondary structure using Jpred 4 (http://www.compbio.dundee.ac.uk/jpred4; Drozdetskiy et al., 2015) and for known motifs using hmmscan (https://www.ebi.ac.uk/Tools/hmmer/search/hmmscan; Finn et al., 2015) and including all HMM databases (Pfam, TIGRFAM, Gene3D, Superfamily and PIRSF).

The *uORF* nucleotide and amino acid sequences were aligned with ClustalW (Larkin et al., 2007; Goujon et al., 2010), using a Multiple Alignment Mode, iterated in each step, and the following parameters: Gap extension: 0, Gap opening: 15, Negative matrix: Off, DNA transition weight: 0.5, Delay divergent seq: 30, Protein weight matrix: Gonnet series, DNA weight matrix: IUB. Identity and IUB quality was used for protein and DNA analysis respectively.

Maximum likehood phylogenetic tree was constructed using the ClustalW alignments, the JTT+I+G model (Jones et al., 1992; Reeves, 1992; Yang, 1993) and 100 bootstrap repeats.

Ribosome footprints analysis

Ribosome Footprints (RF) sequence reads were obtained from Juntawong et al., 2014 (SRX345243, SRX345250, SRX345242, SRX345246); Merchante et al., 2015 (SRX976546, SRX976568, SRX976713, SRX976714), Lei et al., 2015 (SRX845439, SRX845455, SRX847137, SRX847138) and Hsu et al., 2016 (SRX1756756, SRX1756757, SRX1756758, SRX1756759, SRX1756760, SRX1756761, SRX1756762, SRX1756763, SRX1756764, SRX1756765, SRX1756766, SRX1756767). Reads of non-stressed plants were used in this analysis. The coverage was computed for the entire read in RNA-seq samples, and for the nucleotide 13 in each read for Ribo-seq samples. Translation efficiency was calculated as the relationship between the read count in the Ribo-seq sample and the read count in the total RNA sample for each ORF.

RNA profile analysis

The raw reads from the studies analyzed were retrieved from the Gene Expression Omnibus repository. The corresponding accession numbers are: GSE68560 (Mancini et al., 2015), GSE61545 (Liu et al., 2016) and GSE87760 (unpublished work). Reads were first processed to remove adapters and low quality bases using Trimmomatic ver. 0.36 (Bolger et al., 2014) with the suggested options: "LEADING:3 TRAILING:3, SLIDINGWINDOW:4:15 MINLEN:36"; with "MAXINFO:90:0.4" and removing Illumina adapter sequences using the "ILLUMINACLIP" option. The quality of reads

637 before and after trimming was evaluated with FastQC
638 (http://www.bioinformatics.babraham.ac.uk/projects/fastqc/).
639 Processed reads were mapped to the *A. thaliana* genome (TAIR10, Lamesch et al., 2012) using
640 Tophat2 ver. 2.1.1 (Kim et al., 2013) with the default settings. Duplicate reads were removed with
641 MarkDuplicates from the picard toolkit ver. 2.7.0 (http://picarDsourceforge.net/). The results were
642 graphically inspected with IGV (Thorvaldsdottir et al., 2012), which was also used to obtain the
643 Sashimi plots. The comparison of RNA profiles was carried out with the RNAprof software ver.
644 1.2.6 (Tran Vdu et al., 2016), only for the *AtHB1* locus.
645
646 Yeast cell culture, transformation and immunoblotting
647 *Saccharomyces cerevisiae* DF5 *MATα* cells were grown and transformed as described (Capella et al.,
648 2014). Cells were cultured to exponential growth in synthetic minimal medium lacking Trp; one
649 OD_{600} was collected and total cell protein extracts were prepared by TCA precipitation. Proteins
650 were resolved on NuPAGE 12 % gels (Invitrogen), and analyzed by standard immunoblotting
651 techniques using mouse monoclonal antibodies against GFP (B-2; Santa Cruz Biotechnology) and
652 Pgk1 (22C5; Invitrogen), and HRP-Rabbit anti-mouse (Invitrogen).
653
654 Accession numbers:
655 *AtHB1* (At3G01472.1); *ZmHB115* (GRMZM2G021339)
656
657 **List of Supplemental Material**
658 **Figure S1:** Nucleotide sequence alignment of the coding sequences of the peptides listed in Figure
659 1B.
660 **Figure S2:** The context of the second ATG codon fits Kozak rule better
661 **Figure S3:** The length of the uORF is the most conserved feature differing only between
662 monocotyledonous and dicotyledonous plants
663 **Figure S4:** *AtHB1* overexpression is impaired by a mechanism involving siRNA
664 **Figure S5:** *AtHB1* expression is only impaired while *AtHB1* is overexpressed
665 **Figure S6:** The negative regulation exerted by CPuORF33 in not dependent on small RNAs
666 **Figure S7:** *CPuORF33* action is not mediated by NMD
667 **Figure S8:** Transgenic expression of *CPuORF33* does not affect the expression of endogenous
668 *AtHB1*
669 **Figure S9:** Comparative ribosome footprinting profile of *AtHB1* and *AtHB13* transcripts

670 **Figure S10:** The CPuORF33 represses translation in a sequence-dependent manner in **the**
671 heterologous yeast system.
672 **Figure S11:** Comparative ribosome footprinting profile of *AtHB1* transcripts in root vs. shoots.
673 **Figure S12:** *AtHB1* potentially has a secondary TSS that could explain the activity of the differential
674 CPuORF in certain cases
675 **Figure S13:** Histochemical detection of GUS in *35S:native-uORF:GUS* plants grown under different
676 light regimes.
677 **Figure S14:** Ribosome footprinting profile of the transcripts of the maize *AtHB1* homolog *ZmHB115*
678 **Table S1**: Species used in the bioinformatic analysis and the accession number of the corresponding
679 sequence
680 **Table S2**: Oligonucleotides used in this work
681

682 **Acknowledgements**

683 We would like to thank Dr. Federico Ariel for critical reading of the MS.

684

685

686 **Figure legends**

687

688 **Figure 1. The predicted amino acid sequence of the CPuORF33 is highly conserved**
689 **between species**

690 **A**. Schematic representation of *AtHB1* gene. In grey, exons; in light grey, the 5' and 3'UTR; in
691 red, the CPuORF33; and the introns in simple lines.

692 **B**. *Left panel*: Phylogenetic tree constructed using the predicted uORF amino acid sequences of
693 44 AtHB1 homologs from different species, available in public databases. Two main clades can
694 be distinguished: dicotyledonous and monocotyledonous plants. *Right panel*: amino acid
695 sequence alignment.

696 **C.** Amino acid sequence logo of CPuORF33. Sequence logo resulted from the alignment of the
697 uORF amino acid sequences of 44 AtHB1 homologs from different species. Letters height
698 corresponds to the frequency in the alignment.

699

700 **Figure 2. *AtHB1* overexpressor plants bearing a uORF mutated in the putative start codons**
701 **present abnormal phenotypes**

702 **A.** Schematic representation of the native *AtHB1* promoter (*PromAtHB1*) and a mutated version
703 (*PromAtHB1mut*), both including their 5'UTR Two single nucleotides, located within the first
704 two codons of the uORF, were mutated (T→C) and are signaled in green.

705 **B.** Illustrative photographs of 30-day-old Col-0 plants transformed with *PromAtHB1:AtHB1* and
706 *PromAtHB1mut:AtHB1* compared to control plants transformed with an empty *pCambia* vector.

707 **C.** Illustrative photographs of 30-day-old *rdr6-12* mutant plants transformed with
708 *PromAtHB1:AtHB1* and *PromAtHB1mut:AtHB1* compared to control plants transformed with an
709 empty *pCambia*.

710 Two independent transgenic lines for each genotype were analyzed. First (T1) and second (T2)
711 generations are shown in the upper and lower panel, respectively.

712

713 **Figure 3. Mutations in the *CPuORF33* enhance the translation of different downstream**
714 **main ORFs**

715 **A.** Transcript levels of *GUS* in 14-day-old seedlings of Col-0 plants transformed with native
716 *PromAtHB1:GUS* or *PromAtHB1mut:GUS.* Three independent lines of each genotype are

717 shown, paired according to their transcript levels. Transcript levels in whole rosettes were
718 measured by RT-qPCR and the values were normalized with the smaller absolute value using the
719 ΔΔCt method. Y axis is shown in log2 scale.
720 **B.** *GUS* expression analyzed by histochemical detection of GUS enzymatic activity in 14-day-
721 old plants.
722 **C.** GUS activity evaluated by fluorometry in whole rosette protein extracts from the same plants
723 as in A. Error bars: SD of five biological replicates.
724 T-tests were performed and p-values < 0.05 are signaled with asterisks.
725
726 **Figure 4. Ribosome footprinting pattern and mutations in the uORF amino acid sequence**
727 **suggest ribosome stalling at the CPuORF33**
728 **A.** Schematic representation of the constructs used in Arabidopsis transformation, showing the
729 nucleotide (above) and amino acid (below) sequence of the native and mutated uORF. *FS*: Frame
730 shift. *Black*: *35SCaMV promoter*, *white*: *AtHB1 5'UTR, Light blue: CPuORF33, Grey: GUS*
731 *ORF Stars:* Single base modification, *Arrow*: Insertion introduced.
732 **B.** Illustrative photograph of 20-day-old leaves transformed with the indicated constructs and
733 analyzed by GUS histochemisty.
734
735 **Figure 5. CPuORF33 repression action depends on the tissue and environmental condition**
736 Illustrative photographs of organs/tissues of plants revealed by GUS histochemisty. **A**: 5-day-
737 old seedling transformed with *35S:GUS* grown under long day photoperiod (LDP). Bar: 2 mm;
738 **B**: 5-day-old seedling transformed with *35S:native-uORF:GUS* grown under LDP. Bar: 2 mm;
739 **C**: hypocotyl detail of B. Bar: 500 µm; **D**: 10-day-old seedling transformed with *35S:GUS* grown
740 under LDP. Bar: 2 mm; **E**: 10-day-old seedling transformed with *35S:native-uORF:GUS* grown
741 under LDP. Bar: 2 mm; **F**: hypocotyl detail of E. Bar: 500 µm; **G**: root detail of VI. Bar: 200
742 µm; **H**: inflorescence of plants transformed with *35S:GUS.* Bar: 5 mm; **I**: inflorescence of plants
743 transformed with *35S:native-uORF:GUS.* Bar: 5 mM
744 **Figure 6. Light-dependent CPuORF33 repression action in cotylendons is not reverted in**
745 **darkness but avoided by DCMU**
746 Illustrative photographs of seedlings transformed with *35S:GUS* or *35S:native-uORF:GUS* and
747 revealed by GUS histochemistry. **A**: *Left*: 6-day-old seedling transformed with *35S:native-*

748 *uORF:GUS* grown under long photoperiod (LDP). *Center*: 6-day-old seedling transformed with
749 *35S:GUS* grown in darkness. *Right*: 6-day-old seedling transformed with *35S:native-uORF:GUS*
750 grown in darkness. Bar: 2 mm; **B**: *Left*: 8-day-old *35S:native-uORF:GUS* seedlings grown under
751 long photoperiod. *Right*: 6-day-old *35S:native-uORF:GUS* seedlings grown under LDP and then
752 transferred for 2 additional days to darkness. Bar: 2 mm; **C**: *Left*: 6-day-old *35S:native-*
753 *uORF:GUS* seedlings grown in darkness and treated with ethanol during 24 h with ethanol under
754 LDP. *Right*: 6-day-old *35S:native-uORF:GUS* seedlings grown in darkness and treated during 24
755 h with 50 μM DCMU under LDP. Bar: 2 mm
756
757 **Figure 7. The uORF of maize AtHB1' homolog functions as a translational repressor**
758 **A**: Illustrative photographs of 14-day old plants revealed by GUS histochemisty. Left
759 photograph: Arabidopsis plants transformed with *35S:GUS* grown under long photoperiod. Right
760 photographs: three independent lines of Arabidopsis plants transformed with
761 *35S:maize5'UTR:GUS* grown under long photoperiod. Bar: 500 μm.
762
763 **Figure 8. Expression levels of *AtHB1* are fine-tuned due to the detrimental effects for plant**
764 **reproduction and survival generated by its overexpression**
765 **A.** Hypocotyl length of plants grown under short photoperiod for 5 days. Control plants of Col-0
766 and *rdr6-12* backgrounds are shown as well as the same plants transformed with
767 *PromAtHB1:AtHB1* (*PromAtHB1:At1*) and *PromAtHB1mut:AtHB1* (*PromAtHB1mut: At1*). Two
768 independent lines for each genotype are shown. An ANOVA test was performed and pair-wise
769 differences were evaluated with a Tukey *post hoc* test; different groups were marked with letters
770 at 0.05 significance level.
771 **B.** Illustrative photographs of *rdr6-12* plants transformed with *PromAtHB1:AtHB1* and
772 *PromAtHB1mut:AtHB1*. **I.** 25-day-old rosette leaves of control and transformed plants. Four
773 independent lines are shown for each genotype. **II.** Front photograph of the same plants as in I
774 **III** Flowers of 40-day-old plants. **IV**. Siliques of the same plants.
775
776
777
778

779 **Legends to Supplemental Figures**

780

781 **Figure S1. Nucleotide sequence alignment of the coding sequences of the peptides listed in**
782 **Figure 1B.**

783

784 **Figure S2. The context of the second ATG codon fits Kozak rule better**

785 A fragment of the mRNA encoding the uORFs, as presented in Figure 1C, is displayed to
786 highlight the sequence context around the starting codon. For sequences with two initial
787 methionines the first ATG was called ATG1 and the second, ATG2. A position count matrix
788 shows the number of each nucleotide in the alignment whereas their location relative to each
789 ATG is indicated below.

790

791 **Figure S3. The length of the uORF is the most conserved feature differing only between**
792 **monocotyledonous and dicotyledonous plants**

793 **A**. Distribution of the distances comprised between the predicted stop codon of the uORF and the
794 start codon of the main ORF (mORF).

795 **B**. Distribution of the distances comprised between the predicted 5' cap (CAP) site and the start
796 codon of the uORF

797 **C**. Distribution of the uORF length depending on the species

798 **D.** Percentage of species in which the uORF and the mORF are in frame

799 Forty-four uORF sequences from different species were used for the analysis

800

801 **Figure S4. *AtHB1* overexpression is impaired by a mechanism involving siRNA**

802 **A.** *AtHB1* relative transcript levels in 30-day-old Col-0 plants transformed with the indicated
803 construction. Eight single-copy independent lines of each genotype are shown. Black: T1 plants,
804 White: T2 plants. All the values were normalized with the one obtain in Col-0 plants transformed
805 with *pCambia* using the ΔΔCt method.

806 **B.** *AtHB1* relative transcript levels in 30-day-old *rdr6-12* plants transformed with the indicated
807 construction. Eight single-copy independent lines of each genotype are shown. Black: T1 plants,
808 White: T2 plants. All the values were normalized with the one obtain in *rdr6* plants transformed
809 with *pCambia* using the ΔΔCt method.

C. Mean value of *AtHB1* transcript levels in the T1 plants showed in A and B. Values were normalized with the one obtain in Col-0 or *rdr6-12* plants, respectively, transformed with *pCambia* using the ΔΔCt method. In A., B. and C. the y axis is shown in log2 scale. A two-way ANOVA test was performed and no differences were detected at a significance level of 0.05.

Figure S5. *AtHB1* expression is only impaired while *AtHB1* is overexpressed

Transcript levels of *AtHB1* in 14-day-old Col-0 and *rdr6-12* plants grown under normal conditions. Values were normalized with the one obtain in Col-0 plants using the ΔΔCt method. Y axis is shown in log 2 scale T-tests were performed and p-values < 0.05 are signaled with asterisks.

Figure S6. The negative regulation exerted by CPuORF33 in not dependent on small RNAs

A. Transcript levels of *GUS* in 14-day-old seedlings of *rdr6-12* plants transformed with *PromAtHB1:GUS* or *PromAtHB1mut:GUS* Transcript levels in independent transgenic lines were randomly evaluated and normalized with the value measured in the line exhibiting the lowest *GUS* transcript level using the ΔΔCt method with the *Actin* transcripts levels (*ACTIN2* and *ACTIN8*). Numbers in the x axis correspond to each independent line name. The y axis is shown in log2 scale. An ANOVA test was performed and pair-wise differences were evaluated with a Tukey *post hoc* test; different groups were marked with letters at 0.05 significance level.
B. GUS expression analyzed by histochemical detection of GUS enzymatic activity in 14-day-old plants of the same lines showed above.

Figure S7. *CPuORF33* action is not mediated by NMD

Transcript levels of *AtHB1* in 14-day-old Col-0, *upf1-5* and *upf3-1* plants. Values were normalized with the one obtain in Col-0 plants using the ΔΔCt method. Y axis is shown in log2 scale. An ANOVA test was performed and pair-wise differences were evaluated with a Tukey *post hoc* test; different groups were marked with letters at 0.05 significance level. T-tests were performed and p-values < 0.05 are signaled with asterisks.

Figure S8. Transgenic expression of *CPuORF33* does not affect the expression of endogenous *AtHB1*

Transcript levels of *AtHB1* in 30-day-old *rdr6-12* plants transformed with *PromAtHB1:AtHB1* or *PromAtHB1mut:AtHB1*. Three independent lines of each genotype were measure. Total *AtHB1* transcript levels were obtained using oligonucleotides annealing in the *CDS* region, while endogenous *AtHB1* levels were obtain using oligonucleotides annealing in the *3'UTR* region. All the values were normalized with the one obtain in *rdr6-12* plants transformed with *pCambia* using the ΔΔCt method. The y axis is shown in log 2 scale. T-tests were performed between genotypes for total *AtHB1* vs total *AtHB1*, and for endogenous *AtHB1* vs endogenous *AtHB1*. There were no differences at a significance level of 0.05

Figure S9. Comparative ribosome footprinting profile of *AtHB1* and *AtHB13* transcripts

A. RNA-seq coverage and ribosome footprints (P-site) of *AtHB1* transcript in shoots from 4-day-old seedlings (Hsu et al., 2016). *Upper panel*: Coverage of RNA-seq reads. *Lower panel*: Ribosome occupancy. Light blue: *CPuORF33*; Grey: mORF; *white*: 5' and 3'UTR. The relative frequency was calculated as the depth in relation to the sum over whole transcript.

B. RNA-seq coverage and ribosome footprints (P-site) of *AtHB1* transcript in 7-day-old seedlings (Juntawong et al, 2014). *Upper panel*: Coverage of RNA-seq reads.*Lower panel*: Ribosome occupancy.

C. RNA-seq coverage and ribosome footprints (P-site) of *AtHB1* transcript in 4-day-old seedlings (Merchante et al., 2015). *Upper panel*: Coverage of RNA-seq reads. *Lower panel*: Ribosome occupancy.

D. RNA-seq coverage and ribosome footprints (P-site) of *AtHB13* transcript in 4-day-old seedlings (Hsu et al, 2016). Upper panel: Coverage of RNA-seq reads. Lower panel: Ribosome occupancy. Light blue: uORF; Grey: mORF; white: 5' and 3' UTR.

Figure S10. The CPuORF33 represses translation in a sequence-dependent manner in the heterologous yeast system.

A. Schematic representation of the constructs used in *Saccharomyces cerevisiae* transformation, showing the nucleotide (above) and amino acid (below) sequence of the native and mutated uORF. Changes in the amino acid sequence with respect to the native uORF are highlighted in red. *FS*: Frame shift, *Black*: *ADH* promoter, *White*: *5'UTR*, *Light blue*: *CPuORF33*, *Green*:

871 *yeGFP ORF*, Stars: Single base modification, *Arrow*: Insertion introduced or nucleotide
872 removed.
873 **B.** Expression levels of GFP analyzed by immunobloting of yeast transformed with the indicated
874 genetic constructs. Pgk1 serves as a loading control.
875
876 **Figure S11. Comparative ribosome footprinting profile of *AtHB1* transcripts in root vs.**
877 **shoots.**
878 **A**. RNA-seq coverage and ribosome footprints (P-site) of *AtHB1* transcript in shoots (*upper*
879 *panel*) and roots (*lower panel*) from 4-day-old seedlings (Hsu et al, 2016). Light blue:
880 CPuORF33; Grey: mORF; white: 5' and 3'UTR **B.** Relation between mORF and uORF
881 translation efficiency in 4-day-old seedlings (Hsu et al., 2016).
882
883 **Figure S12. *AtHB1* potentially has a secondary TSS that could explain the activity of the**
884 **differential CPuORF in certain cases**
885 **A.** Representation of the *AtHB1* locus. Coding regions are depicted with broad boxes and introns
886 are shown as lines with arrowheads indicating the sense of transcription. The transcription start
887 sites (TSSs) defined by Morton et al (2014) are highlighted with the names given by the authors.
888 Red arrows indicate target sites of oligonucleotides used in the RT-qPCR assay. **B.** Sashimi plots
889 showing the RNA coverage profile along the *AtHB1* locus, used for mapping the reads, for the
890 rosette and root samples from Grillet and Schmidt (GEO accession GSE87760). **C.** Output graph
891 from the RNAprof (Tran et al, 2016) program contrasting the RNA coverage profiles. The region
892 that presented a significant difference between tissues (p-value 2.9e-4) is highlighted over the
893 profile. The location of the uORF and the TSS from Morton et al. (2014) have been added to the
894 graph. **D.** Sashimi plots obtained with sequencing data from Mancini et al. (2016) showing the
895 RNA coverage profile along the *AtHB1* locus. In this case no differences in the profile was found
896 with RNAprof when comparing dark and light grown plants. **E.** The upper panel shows the
897 Sashimi plots obtained with sequencing data from Liu et al. (2016) showing the RNA coverage
898 profile along the AtHB1 locus. The lower panel shows the output of running RNAprof for the
899 comparison of the RNA coverage profiles. The region presenting a differential profile between
900 tissues is highlighted and annotated with coordinates, score (fold-change) and p-value
901 information on top.

902

903 **Figure S13. Histochemical detection of GUS in *35S:native-uORF:GUS* plants grown under**
904 **different light regimes.** Panels **A**, **B** and **C** show 8-day-old *35S:native-uORF:GUS* seedlings
905 grown in: darkness (**A,** bar: 2 mm), 6 days in darkness and then transferred to long day
906 photoperiod (LDP) for 2 additional days; (**B**, bar: 0.5 mm); and 6 days in darkness, then exposed
907 to light for 1 h and then, transferred to darkness for 2 additional days (**C**, bar: 2 mm). Panels **D**,
908 **E** and **F** show 20-day-old seedling of: *35S:GUS* grown under LDP (**D**, bar: 2 mm); *35S:native-*
909 *uORF:GUS* grown under LDP (**E**, bar: 2 mm); and *35S:native-uORF:GUS* grown under LDP for
910 15 days and then transferred to darkness for 5 additional days (**F**, bar: 2 mm). Panels **G**, **H** and **I**
911 show 6-day-old *35S:native-uORF:GUS* seedlings grown in: white light and LDP (N, bar: 1 mm);
912 blue light (480 nm) and LDP (**H**, bar: 1 mm); and red light (680 nm) and LDP (**I**, bar: 2 mm).

913

914 **Figure S14. Ribosome footprinting profile of the transcripts of the maize *AtHB1* homolog**
915 ***ZmHB115***

916 RNA-seq coverage and ribosome footprintings (P-site) of *ZmHB115* transcript in 14-day-old
917 seedlings (Lei et al., 2015). *Upper panel*: Coverage of RNA-seq reads. *Lower panel*: Ribosome
918 occupancy. Light blue: uORF; Grey: mORF; white: 5' and 3'UTR.

919

920

Parsed Citations

Alatorre-Cobos F, Cruz-Ramírez A, Hayden CA, Pérez-Torres CA, Chauvin AL, Ibarra-Laclette E, Alva-Cortés E, Jorgensen RA, Herrera-Estrella L (2012) Translational regulation of Arabidopsis XIPOTL1 is modulated by phosphocholine levels via the phylogenetically conserved upstream open reading frame 30. J Exp Bot 63:5203-5221

Pubmed: Author and Title
CrossRef: Author and Title
Google Scholar: Author Only Title Only Author and Title

Altschul SF, Gish W, Miller W, Myers EW, Lipman DJ (1990) Basic local aignment search tool. J Mol Biol 215:403-410

Pubmed: Author and Title
CrossRef: Author and Title
Google Scholar: Author Only Title Only Author and Title

Aoyama T, Dong CH Wu Y, Carabelli M, Sessa G, Ruberti I, Morelli G, Chua, NH (1995) Ectopic expression of the Arabidopsis transcriptional activator Athb-1 alters leaf cell fate in tobacco. Plant Cell 7:1773-1785

Pubmed: Author and Title
CrossRef: Author and Title
Google Scholar: Author Only Title Only Author and Title

Arce AL, Raineri J, Capella M, Cabello JV, Chan RL (2011) Uncharacterized conserved motifs outside the HD-Zip domain in HD-Zip subfamily I transcription factors; a potential source of functional diversity. BMC Plant Biol 11:42

Pubmed: Author and Title
CrossRef: Author and Title
Google Scholar: Author Only Title Only Author and Title

Bender J, Fink GR (1998) A Myb homologue, ATR1, activates tryptophan gene expression in Arabidopsis. Proc Natl Acad Sci USA 95:5655-5660

Pubmed: Author and Title
CrossRef: Author and Title
Google Scholar: Author Only Title Only Author and Title

Bolger AM, Lohse M, Usadel B (2014) Trimmomatic: A flexible trimmer for Illumina Sequence Data. Bioinformatics 30:2114-2120

Pubmed: Author and Title
CrossRef: Author and Title
Google Scholar: Author Only Title Only Author and Title

Calvo SE, Pagliarini DJ, Mootha VK (2009) Upstream open reading frames cause widespread reduction of protein expression and are polymorphic among humans. Proc Natl Acad Sci USA 106:7507-7512

Pubmed: Author and Title
CrossRef: Author and Title
Google Scholar: Author Only Title Only Author and Title

Capella M, Ré DA, Arce AL, Chan RL (2014) Plant homeodomain-leucine zipper I transcription factors exhibit different functional AHA motifs that selectively interact with TBP or/and TFIIB. Plant Cell Rep 33:955-967

Pubmed: Author and Title
CrossRef: Author and Title
Google Scholar: Author Only Title Only Author and Title

Capella M, Ribone PA, Arce AL, Chan RL (2015a) Homeodomain–leucine zipper transcription factors: structural features of these proteins, unique to plants. In Plant Transcription Factors: Evolutionary, Structural and Functional Aspects. (Eds: González, DH) Elsevier, Amsterdam, The Netherlands, 113-126

Pubmed: Author and Title
CrossRef: Author and Title
Google Scholar: Author Only Title Only Author and Title

Capella M, Ribone PA, Arce AL, Chan RL (2015b) Arabidopsis thaliana HomeoBox 1 (AtHB1), a Homedomain-Leucine Zipper I (HD-Zip I) transcription factor, is regulated by PHYTOCHROME-INTERACTING FACTOR 1 to promote hypocotyl elongation. New Phytol 207:669-682

Pubmed: Author and Title
CrossRef: Author and Title
Google Scholar: Author Only Title Only Author and Title

Clough SJ, Bent AF (1998) Floral dip: a simplified method for Agrobacterium-mediated transformation of Arabidopsis thaliana. Plant J 16:735-743

Pubmed: Author and Title
CrossRef: Author and Title
Google Scholar: Author Only Title Only Author and Title

Combier JP, de Billy F, Gamas P, Niebel A, Rivas S (2008) Trans-regulation of the expression of the transcription factor MtHAP2-1 by a uORF controls root nodule development. Genes Dev 22:1549-1559

Pubmed: Author and Title
CrossRef: Author and Title
Google Scholar: Author Only Title Only Author and Title

Drozdetskiy A, Cole C, Procter J, Barton GJ (2015) JPred4: a protein secondary structure prediction server. Nucleic Acids Res 43:W389-394
Pubmed: Author and Title
CrossRef: Author and Title
Google Scholar: Author Only Title Only Author and Title

Ebina I, Takemoto-Tsutsumi M, Watanabe S, Koyama H, Endo Y, Kimata K, Igarashi T, Murakami K, Kudo R, Ohsumi A, Noh AL, Takahashi H, Naito S, Onouchi H (2015) Identification of novel Arabidopsis thaliana upstream open reading frames that control expression of the main coding sequences in a peptide sequence-dependent manner. Nucleic Acids Res 43:1562-1576
Pubmed: Author and Title
CrossRef: Author and Title
Google Scholar: Author Only Title Only Author and Title

Finn RD, Clements J, Arndt W, Miller BL, Wheeler TJ, Schreiber F, Bateman A, Eddy SR (2015) HMMER web server: 2015 update. Nucleic Acids Res 43:W30-38
Pubmed: Author and Title
CrossRef: Author and Title
Google Scholar: Author Only Title Only Author and Title

Goujon M, McWilliam H, Li W, Valentin F, Squizzato S, Paern J, Lopez R (2010) A new bioinformatics analysis tools framework at EMBL-EBI. Nucleic Acids Res W695-699
Pubmed: Author and Title
CrossRef: Author and Title
Google Scholar: Author Only Title Only Author and Title

Guerrero-González ML, Rodríguez-Kessler M, Jiménez-Bremont JF (2014) uORF, a regulatory mechanism of the Arabidopsis polyamine oxidase 2. Mol Biol Rep 41:2427-2443
Pubmed: Author and Title
CrossRef: Author and Title
Google Scholar: Author Only Title Only Author and Title

Guerrero-González ML, Ortega-Amaro MA, Juárez-Montiel M, Jiménez-Bremont JF (2016) Arabidopsis polyamine oxidase-2 uORF is required for downstream translational regulation. Plant Physiol Biochem 108:381-390
Pubmed: Author and Title
CrossRef: Author and Title
Google Scholar: Author Only Title Only Author and Title

Hanfrey C, Elliott KA, Franceschetti M, Mayer MJ, Illingworth C, Michael AJ (2005) A dual upstream open reading frame-based autoregulatory circuit controlling polyamine-responsive translation. J Biol Chem 280:39229-39237
Pubmed: Author and Title
CrossRef: Author and Title
Google Scholar: Author Only Title Only Author and Title

Hayashi N, Sasaki S, Takahashi H, Yamashita Y, Naito S, Onouchi H (2017) Identification of Arabidopsis thaliana upstream open reading frames encoding peptide sequences that cause ribosomal arrest. Nucleic Acid Res gkx528. doi: 10.1093/nar/gkx528
Pubmed: Author and Title
CrossRef: Author and Title
Google Scholar: Author Only Title Only Author and Title

Hayden CA, Jorgensen RA (2007) Identification of novel conserved peptide uORF homology groups in arabidopsis and rice reveals ancient eukaryotic origin of select groups and preferential association with transcription factor-encoding genes. BMC Biol 5:32
Pubmed: Author and Title
CrossRef: Author and Title
Google Scholar: Author Only Title Only Author and Title

Hayden CA, Bosco G (2008) Comparative genomic analysis of novel conserved peptide upstream open reading frames in drosophila melanogaster and other dipteran species. BMC Genomics 9:61
Pubmed: Author and Title
CrossRef: Author and Title
Google Scholar: Author Only Title Only Author and Title

Henriksson E, Olsson ASB, Johannesson H, Johansson H, Hanson J, Engström P, Söderman E (2005) Homeodomain Leucine Zipper class I genes in Arabidopsis expression patterns and phylogenetic relationships. Plant Physiol 139:509-518
Pubmed: Author and Title
CrossRef: Author and Title
Google Scholar: Author Only Title Only Author and Title

Higuchi R, Krummel B, Saiki RK (1988) A general method of in vitro preparation and specific mutagenesis of DNA fragments: study of protein and DNA interactions. Nucleic Acids Res 16:7351–7367
Pubmed: Author and Title
CrossRef: Author and Title
Google Scholar: Author Only Title Only Author and Title

Hofer J, Turner L, Moreau C, Ambrose M, Isaac P, Butcher S, Weller J, Dupin A, Dalmais M, Le Signor C, Bendahmane A, Ellis N (2009) Tendril-Less regulates tendril formation in pea leaves. Plant Cell 21:420-428

Pubmed: Author and Title
CrossRef: Author and Title
Google Scholar: Author Only Title Only Author and Title

Hou CY, Lee WC, Chou HC, Chen AP, Chou SJ, Chen HM (2016) Global analysis of truncated RNA ends reveals new insights into ribosome stalling in plants. Plant Cell 28: 2398–2416

Pubmed: Author and Title
CrossRef: Author and Title
Google Scholar: Author Only Title Only Author and Title

Hsu PY, Calviello L, Larry Wud H-Y, Li F-W, Rothfels CJ, Ohlerb U, Benfey PN (2016) Super-resolution ribosome profiling reveals unannotated translation events in Arabidopsis. Proc Natl Acad Sci USA 113: E7126–E7135

Pubmed: Author and Title
CrossRef: Author and Title
Google Scholar: Author Only Title Only Author and Title

Imai A, Hanzawa Y, Komura M, Yamamoto KT, Komeda Y, Takahashi T (2006) The dwarf phenotype of the Arabidopsis acl5 mutant is suppressed by a mutation in an upstream ORF of a bHLH gene. Development 133:3575-3585

Pubmed: Author and Title
CrossRef: Author and Title
Google Scholar: Author Only Title Only Author and Title

Ingolia NT, Ghaemmaghami S, Newman JRS, Weissman JS (2009) Genome-wide analysis in vivo of translation with nucleotide resolution using ribosome profiling. Science 324:218-223

Pubmed: Author and Title
CrossRef: Author and Title
Google Scholar: Author Only Title Only Author and Title

Ito K, Chiba S (2013) Arrest peptides: cis -acting modulators of translation. Annu Rev Biochem 82:171-202

Pubmed: Author and Title
CrossRef: Author and Title
Google Scholar: Author Only Title Only Author and Title

Ivanov IP, Atkins JF, Michael AJ (2010) A profusion of upstream open reading frame mechanisms in polyamine-responsive translational regulation. Nucleic Acids Res 38:353-359

Pubmed: Author and Title
CrossRef: Author and Title
Google Scholar: Author Only Title Only Author and Title

Jefferson RA, Kavanagh TA, Bevan MW (1987) GUS fusions: beta-glucuronidase as a sensitive and versatile gene fusion marker in higher plants. EMBO J 6:3901-3907

Pubmed: Author and Title
CrossRef: Author and Title
Google Scholar: Author Only Title Only Author and Title

Jones DT, Taylor WR, Thornton JM (1992) The rapid generation of mutation data matrices from protein sequences. Bioinformatics 8:275-282

Pubmed: Author and Title
CrossRef: Author and Title
Google Scholar: Author Only Title Only Author and Title

Jorgensen RA, Dorantes-Acosta AE (2012) Conserved peptide upstream open reading frames are associated with regulatory genes in angiosperms. Front Plant Sci 3:1-11

Pubmed: Author and Title
CrossRef: Author and Title
Google Scholar: Author Only Title Only Author and Title

Juntawong P, Girke T, Bazin J, Bailey-Serres J (2014) Translational dynamics revealed by genome-wide profiling of ribosome footprints in Arabidopsis. Proc Natl Acad Sci USA 111:E203-E212.

Pubmed: Author and Title
CrossRef: Author and Title
Google Scholar: Author Only Title Only Author and Title

Kalyna M, Simpson CG, Syed NH, Lewandowska D, Marquez Y, Kusenda B, Marshall J, Fuller J, Cardle L, McNicol J, Dinh HQ, Barta A, Brown JWS (2012) Alternative splicing and nonsense-mediated decay modulate expression of important regulatory genes in Arabidopsis. Nucleic Acids Res 40:2454-2469

Pubmed: Author and Title
CrossRef: Author and Title
Google Scholar: Author Only Title Only Author and Title

Katayama H, Iwamoto K, Kariya Y, Asakawa T, Kan T, Fukuda H, Ohashi-Ito K (2015) A negative feedback loop controlling bHLH complexes is involved in vascular cell division and differentiation in the root apical meristem. Curr Biol 25:3144–3150

Pubmed: Author and Title
CrossRef: Author and Title
Google Scholar: Author Only Title Only Author and Title

Kim D, Pertea G, Trapnell C, Pimentel H, Kelley R, Salzberg SL (2013) TopHat2: accurate alignment of transcriptomes in the presence of insertions, deletions and gene fusions. Genome Biol 14:R36
Pubmed: Author and Title
CrossRef: Author and Title
Google Scholar: Author Only Title Only Author and Title

Kozak M (1986) Point mutations define a sequence flanking the AUG initiator codon that modulates translation by eukaryotic ribosomes. Cell 44:283-292
Pubmed: Author and Title
CrossRef: Author and Title
Google Scholar: Author Only Title Only Author and Title

Kozak M (1987) Effects of intercistronic length on the efficiency of reinitiation by eucaryotic ribosomes. Mol Cell Biol 7:3438-3445
Pubmed: Author and Title
CrossRef: Author and Title
Google Scholar: Author Only Title Only Author and Title

Kozak M (2002) Pushing the limits of the scanning mechanism for initiation of translation. Gene 299:1-34
Pubmed: Author and Title
CrossRef: Author and Title
Google Scholar: Author Only Title Only Author and Title

Kwak SH, Lee SH (2001) The regulation of ornithine decarboxylase gene expression by sucrose and small upstream open reading frame in tomato (Lycopersicon Esculentum Mill). Plant Cell Physiol 42:314-323
Pubmed: Author and Title
CrossRef: Author and Title
Google Scholar: Author Only Title Only Author and Title

Laing WA, Martínez-Sánchez M, Wright MA, Bulley SM, Brewster D, Dare AP, Rassam M, Wang D, Storey R, Macknight RC, Hellens RP (2015) An upstream open reading frame is essential for feedback regulation of ascorbate biosynthesis in Arabidopsis. Plant Cell 27:772-786
Pubmed: Author and Title
CrossRef: Author and Title
Google Scholar: Author Only Title Only Author and Title

Lamesch P, Berardini TZ, Li D, Swarbreck D, Wilks C, Sasidharan R, Muller R, Dreher K, Alexander DL, Garcia-Hernandez M, Karthikeyan AS, Lee CH, Nelson WD, Ploetz L, Singh S, Wensel A, Huala E (2012) The Arabidopsis Information Resource (TAIR): Improved gene annotation and new tools. Nucleic Acids Res 40 (Database issue): D1202-1210
Pubmed: Author and Title
CrossRef: Author and Title
Google Scholar: Author Only Title Only Author and Title

Larkin MA, Blackshields G, Brown NP, Chenna R, McGettigan PA, McWilliam H, Valentin F, Wallace IM, Wilm A, Lopez R, Thompson JD, Gibson TJ, Higgins DG (2007) Clustal W. and Clustal X version 2.0. Bioinformatics 23:2947-2948.
Pubmed: Author and Title
CrossRef: Author and Title
Google Scholar: Author Only Title Only Author and Title

Lei L, Shi J, Chen J, Zhang M, Sun S, Xie S, Li X, Zeng B, Peng L, Hauck A, Zhao H, Song W, Fan Z, Lai, J (2015) Ribosome profiling reveals dynamic translational landscape in maize seedlings under drought stress. Plant J 84:1206-1218
Pubmed: Author and Title
CrossRef: Author and Title
Google Scholar: Author Only Title Only Author and Title

Liu J, Deng S, Wang H, Ye J, Wu HW, Sun HX, Chua, NH (2016) CURLY LEAF Regulates gene sets coordinating seed size and lipid biosynthesis. Plant Physiol 171:424-436
Pubmed: Author and Title
CrossRef: Author and Title
Google Scholar: Author Only Title Only Author and Title

Manavella PA, Arce AL, Dezar CA, Bitton F, Renou JP, Crespi M, Chan, RL (2006) Cross-talk between ethylene and drought signalling pathways is mediated by the sunflower Hahb-4 transcription factor. Plant J 48:125-137
Pubmed: Author and Title
CrossRef: Author and Title
Google Scholar: Author Only Title Only Author and Title

Mancini E, Sanchez SE, Romanowski A, Schlaen RG, Sanchez-Lamas M, Cerdán PD, Yanovsky MJ (2016) Acute Effects of Light on Alternative Splicing in Light-Grown Plants. Photochem Photobiol 92:126-133
Pubmed: Author and Title
CrossRef: Author and Title
Google Scholar: Author Only Title Only Author and Title

Matzke MA, Matzke AJM, Pruss GJ, Vance VB (2001) RNA-based silencing strategies in plants. Curr Opin Genet Dev 11:221-227
Pubmed: Author and Title
CrossRef: Author and Title

Google Scholar: Author Only Title Only Author and Title

Merchante C, Brumos J, Yun J, Hu Q, Spencer KR, Enríquez P, Binder BM, Heber S, Stepanova AN, Alonso JM (2015) Gene-Specific translation regulation mediated by the hormone-signaling molecule EIN2. Cell 163:684-697
Pubmed: Author and Title
CrossRef: Author and Title
Google Scholar: Author Only Title Only Author and Title

Moreno Piovano GS, Moreno JE, Cabello JV, Arce AL, Otegui ME, Chan, RL (2017) A role for LAX2 in regulating xylem development and lateral-vein symmetry in the leaf. Ann Bot doi: 10.1093/aob/mcx091
Pubmed: Author and Title
CrossRef: Author and Title
Google Scholar: Author Only Title Only Author and Title

Morton T, Petricka J, Corcoran DL, Li S, Winter CM, Carda A, Benfey PN, Ohler U, Megraw M (2014) Paired-end analysis of transcription start sites in Arabidopsis reveals plant-specific promoter signatures. Plant Cell 26:2746-2760
Pubmed: Author and Title
CrossRef: Author and Title
Google Scholar: Author Only Title Only Author and Title

Nagalakshmi U, Wang Z, Waern K, Shou C, Raha D, Gerstein M, Snyder M (2008) The transcriptional landscape of the yeast genome defined by RNA sequencing. Science 320:1344-1349
Pubmed: Author and Title
CrossRef: Author and Title
Google Scholar: Author Only Title Only Author and Title

Nilsson OB, Hedman R, Marino J, Wickles S, Bischoff L, Johansson M, Müller-Lucks A, Trovato F, Puglisi JD, O'Brien EP, Beckmann R, von Heijne G (2015) Cotranslational protein folding inside the ribosome exit tunnel. Cell Rep 12:1533-1540
Pubmed: Author and Title
CrossRef: Author and Title
Google Scholar: Author Only Title Only Author and Title

Peragine A, Yoshikawa M, Wu G, Albrecht HL, Poethig RS (2004) SGS3 and SGS2/SDE1/RDR6 Are Required for Juvenile Development and the Production of Trans-Acting siRNAs in Arabidopsis. Genes Dev 18:2368-2379
Pubmed: Author and Title
CrossRef: Author and Title
Google Scholar: Author Only Title Only Author and Title

Pfaffl MW (2001) A new mathematical model for relative quantification in real-time RT-PCR. Nucleic Acids Res 29:e45
Pubmed: Author and Title
CrossRef: Author and Title
Google Scholar: Author Only Title Only Author and Title

Pumplin N, Sarazin A, Jullien PE, Bologna NG, Oberlin S, Voinnet O (2016) DNA methylation influences the expression of DICER-LIKE4 isoforms, which encode proteins of alternative localization and function. Plant Cell 28:2786-2804
Pubmed: Author and Title
CrossRef: Author and Title
Google Scholar: Author Only Title Only Author and Title

Rahmani F, Hummel M, Schuurmans J, Wiese-Klinkenberg A, Smeekens S, Hanson, J (2009) Sucrose control of translation mediated by an upstream open reading frame-encoded peptide. Plant Physiol 150:1356-1367
Pubmed: Author and Title
CrossRef: Author and Title
Google Scholar: Author Only Title Only Author and Title

Rajeevkumar S, Anunanthini P, Sathishkumar R (2015) Epigenetic silencing in transgenic plants. Front Plant Sci 6:693
Pubmed: Author and Title
CrossRef: Author and Title
Google Scholar: Author Only Title Only Author and Title

Re DA, Capella M, Bonaventure G, Chan, RL (2014) Arabidopsis AtHB7 and AtHB12 evolved divergently to fine tune processes associated with growth and responses to water stress. BMC Plant Biol 14:150
Pubmed: Author and Title
CrossRef: Author and Title
Google Scholar: Author Only Title Only Author and Title

Reeves JH (1992) Heterogeneity in the substitution process of amino acid sites of proteins coded for by mitochondrial DNA. J Mol Evol 35:17-31
Pubmed: Author and Title
CrossRef: Author and Title
Google Scholar: Author Only Title Only Author and Title

Ribichich KF, Arce AL, Chan, RL (2014) Coping with drought and salinity stresses: role of transcription factors in crop improvemenT In Climate Change and Plant Abiotic Stress Tolerance (Eds.: Tuteja N y Gill SS) Wiley-VCH Verlag GmbH & CO KGaA, Weinheim, Germany, pp: 641-684

Ribone PA, Capella M, Arce AL, Chan RL (2015a) What do we know about homeodomain-leucine zipper I transcription factors? Functional and biotechnological considerations. In Plant Transcription Factors: Evolutionary, Structural and Functional Aspects (Eds: González, DH) Elsevier, Amsterdam, The Netherlands, pP 343-356
Pubmed: Author and Title
CrossRef: Author and Title
Google Scholar: Author Only Title Only Author and Title

Ribone PA, Capella M, Chan, RL (2015b) Functional characterization of the homeodomain leucine zipper I transcription factor AtHB13 reveals a crucial role in Arabidopsis development. J Exp Bot 66:5929-5943
Pubmed: Author and Title
CrossRef: Author and Title
Google Scholar: Author Only Title Only Author and Title

Rice P, Longden I, Bleasby A (2000) EMBOSS: the European Molecular Biology Open Software Suite. Trends Genet 16:276-277
Pubmed: Author and Title
CrossRef: Author and Title
Google Scholar: Author Only Title Only Author and Title

Romani F, Ribone PA, Capella M, Miguel VN, Chan RL (2015) A matter of quantity: common features in the drought response of transgenic plants overexpressing HD-Zip I transcription factors. Plant Sci 251:139-154
Pubmed: Author and Title
CrossRef: Author and Title
Google Scholar: Author Only Title Only Author and Title

Sakuma S, Pourkheirandish M, Hensel G, Kumlehn J, Stein N, Tagiri A, Yamaji N, Ma JF, Sassa H, Koba T, et al. (2013) Divergence of expression pattern contributed to neofunctionalization of duplicated HD-Zip I transcription factor in barley. New Phytol 197:939-948
Pubmed: Author and Title
CrossRef: Author and Title
Google Scholar: Author Only Title Only Author and Title

Saul H, Elharrar E, Gaash R, Eliaz D, Valenci M, Akua T, Avramov M, Frankel N, Berezin I, Gottlieb D, Elazar M, David-Assael O, Tcherkas V, Mizrachi K, Shaul O (2009) The upstream open reading frame of the Arabidopsis AtMHX gene has a strong impact on transcript accumulation through the nonsense-mediated mRNA decay pathway. Plant J 60:1031-1042
Pubmed: Author and Title
CrossRef: Author and Title
Google Scholar: Author Only Title Only Author and Title

Schubert D, Lechtenberg B, Forsbach A, Gils M, Bahadur S, Schmidt R (2004) Silencing in Arabidopsis T-DNA Transformants: The predominant role of a gene-specific RNA sensing mechanism versus position effects. Plant Cell 16:2561-2572
Pubmed: Author and Title
CrossRef: Author and Title
Google Scholar: Author Only Title Only Author and Title

Somers J, Pöyry T, Willis AE (2013) A perspective on mammalian upstream open reading frame function. Int J Biochem Cell Biol 45:1690-1700
Pubmed: Author and Title
CrossRef: Author and Title
Google Scholar: Author Only Title Only Author and Title

Takahashi H, Takahashi A, Naito S, Onouchi, H (2012) BAIUCAS: A novel BLAST-based algorithm for the identification of upstream open reading frames with conserved amino acid sequences and its application to the Arabidopsis thaliana genome. Bioinformatics 28:2231-2241
Pubmed: Author and Title
CrossRef: Author and Title
Google Scholar: Author Only Title Only Author and Title

Tanaka M, Sotta N, Yamazumi Y, Yamashita Y, Miwa K, Murota K, Chiba Y, Hirai MY, Akiyama T, Onouchi H, Naito S, Fujiwara T (2016) The Minimum Open Reading Frame, AUG-Stop, Induces Boron-Dependent Ribosome Stalling and mRNA Degradation. Plant Cell 28:2830-2849
Pubmed: Author and Title
CrossRef: Author and Title
Google Scholar: Author Only Title Only Author and Title

Thorvaldsdottir H, Robinson JT, Mesirov JP (2012) Integrative Genomics Viewer (IGV): High-performance genomics data visualization and exploration. Briefings in Bioinformatics 14:178-192
Pubmed: Author and Title
CrossRef: Author and Title
Google Scholar: Author Only Title Only Author and Title

Tran Vdu T, Souiai O, Romero-Barrios N, Crespi M, Gautheret D (2016) Detection of generic differential RNA processing events from RNA-seq data. RNA Biol 13:59-67
Pubmed: Author and Title
CrossRef: Author and Title
Google Scholar: Author Only Title Only Author and Title

Uchiyama-Kadokura N, Murakami K, Takemoto M, Koyanagi N, Murota K, Naito S, Onouchi H (2014) Polyamine-responsive ribosomal arrest at the stop codon of an upstream open reading frame of the AdoMetDC1 gene triggers nonsense-mediated mRNA decay in Arabidopsis thaliana. Plant Cell Physiol 55:1556-1567
Pubmed: Author and Title
CrossRef: Author and Title
Google Scholar: Author Only Title Only Author and Title

Vaucheret H, Fagard M (2001) Transcriptional gene silencing in plants: targets, inducers and regulators. Trends Genet 17:29-35
Pubmed: Author and Title
CrossRef: Author and Title
Google Scholar: Author Only Title Only Author and Title

von Armin AG, Jia Q, Vaughn JN (2014) Regulation of plant translation by upstream open reading frames. Plant Sci 214:1-12
Pubmed: Author and Title
CrossRef: Author and Title
Google Scholar: Author Only Title Only Author and Title

Vlad D, Kierzkowski D, Rast MI, Vuolo F, Dello Ioio R, Galinha C, Gan X, Hajheidari M, Hay A, Smith RS, et al. (2014) Leaf shape evolution through duplication, regulatory diversification, and loss of a homeobox gene. Science 343:780-783
Pubmed: Author and Title
CrossRef: Author and Title
Google Scholar: Author Only Title Only Author and Title

Wang L, Wessler SR (1998) Inefficient reinitiation is responsible for upstream open reading frame-mediated translational repression of the maize R Gene. Plant Cell 10:1733-1746
Pubmed: Author and Title
CrossRef: Author and Title
Google Scholar: Author Only Title Only Author and Title

Wang W, Vinocur B, Altman A (2003) Plant responses to drought, salinity and extreme temperatures: towards genetic engineering for stress tolerance. Planta 218:1-14
Pubmed: Author and Title
CrossRef: Author and Title
Google Scholar: Author Only Title Only Author and Title

Wiese A, Elzinga N, Wobbes B, Smeekens S (2004) A conserved upstream open reading frame mediates sucrose-induced repression of translation. Plant Cell 16:1717-1729
Pubmed: Author and Title
CrossRef: Author and Title
Google Scholar: Author Only Title Only Author and Title

Yang Z (1993) Maximum-likelihood estimation of phylogeny from DNA sequences when substitution rates differ over sites. Mol Biol Evol 10:1396-1401
Pubmed: Author and Title
CrossRef: Author and Title
Google Scholar: Author Only Title Only Author and Title

Zur H, Tuller T (2013) New universal rules of eukaryotic translation initiation fidelity. PLoS Comput Biol 9:e1003136
Pubmed: Author and Title
CrossRef: Author and Title
Google Scholar: Author Only Title Only Author and Title